Chapter 8
Chemical and Biological Sensors

Chemical and biological sensors are found across a broad range of application areas. An ideal sensor is one with high sensitivity, fast response time, selectivity, and compactness. Achieving this goal is difficult, and current sensor technologies utilize a variety of approaches. As progress in the miniaturization of electronics components is continued, the feasibility of small and inexpensive massive arrays of chemiresistors is a promising approach that might rival more established sensing technologies. Chemiresistors are simple devices where the resistance of a material changes upon exposure to analytes. One aspect of chemiresistors that can benefit from nanomaterials is the sensitivity, because nanomaterials, carbon nanotubes in particular, have a large surface-to-volume ratio. Indeed, a carbon nanotube is entirely a surface material, and its circumference is comparable to the size of many small analytes. Thus, even a single analyte that attaches on the surface of a carbon nanotube can significantly impact the nanotube conductivity. This "single-molecule" detection capability would be difficult to achieve with bulk or thin film materials.

In this chapter, we present the progress that has been made in developing chemical and biological sensors based on monitoring the conductance of carbon nanotubes when exposed to analytes. There are several different physical mechanisms that can lead to changes of the nanotube conductivity in the presence of analytes: charge transfer, changes in electron scattering, contact effects, and capacitance changes. Carbon nanotube field-effect transistors are often utilized as sensitive electronic devices to probe these mechanisms, but sensing with metallic carbon nanotubes has also been explored. One of the first examples demonstrating modulation of the electrical response of carbon nanotubes in the presence of analytes studied the transfer characteristics of carbon nanotube field effect transistors when exposed to NO_2 and NH_3. These gas-sensing experiments were performed by placing a nanotube field effect device in a glass flask with electrical feedthrough, and flowing diluted NH_3 and NO_2 in Ar or air through the flask while measuring the conductance of the nanotube device. Figure 8.1 shows an atomic force microscope image of one device, and the results of the controlled exposure experiments. Clearly, exposure of the device to ammonia significantly decreases the conductance, by a factor of one hundred in this case. Exposure to nitrogen dioxide gives the opposite effect, significantly increasing the conductance when the nanotube device is initially in the OFF state. This behavior is confirmed by measuring the transfer characteristics of the device before and after exposure. As Figure 8.1 indicates, the transfer curve is shifted to more negative values of the gate voltage upon exposure to ammonia, while nitrogen dioxide causes a shift to more positive values of the gate voltage. Thus for ammonia, the large initial conductance at a gate voltage of 0 volt is considerably decreased. For nitrogen dioxide, the small initial conductance at $V_G = +4$ Volts is considerably increased after exposure. These initial experiments clearly demonstrated the potential of carbon nanotubes for chemical sensing, and have spurred

fundamental work to identify the mechanisms that lead to such a large electrical response in carbon nanotubes. We note that the reader will have encountered related mechanisms at the end of Chapter 7 on optoelectronic devices, in the context of optical detection with functionalized carbon nanotubes.

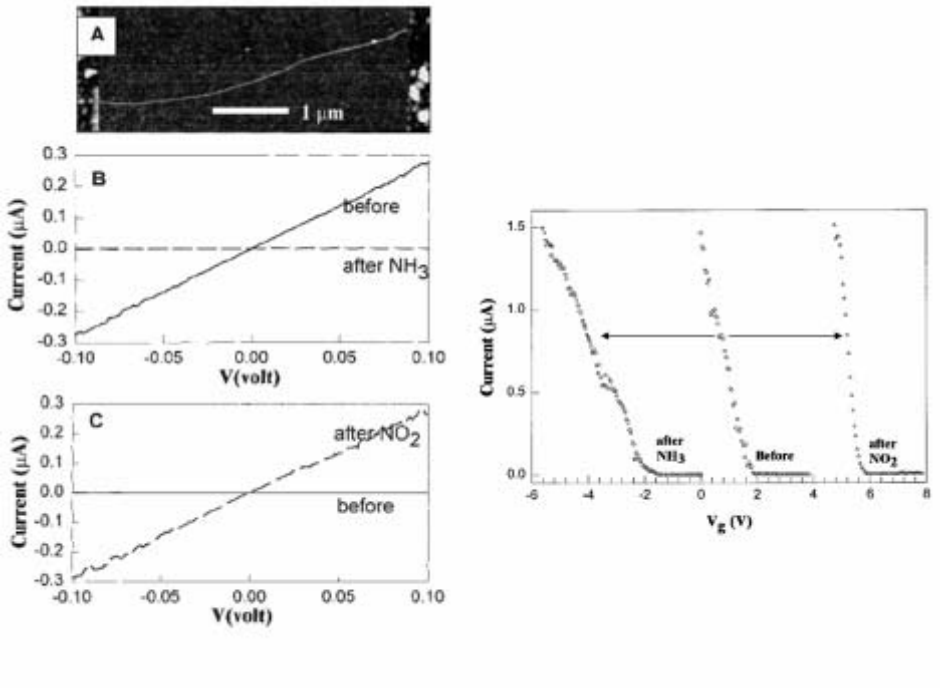

Figure 8.1: Left panels: (1) Atomic force microscope image of a single carbon nanotube in a field-effect device. (B) Current versus gate voltage measured before and after exposure to NH_3. (C) Current versus voltage measured before and after exposure to NO_2. Right panel: Transfer characteristics of the carbon nanotube field-effect transistor before and after exposure to NH_3 and NO_2. Exposure of the device to these analytes leads to a shift of the threshold voltage in the positive or negative direction. *Figures from Ref. [Kon00].*

8.1 Sensing Mechanisms

8.1.1 Charge Transfer

Near the threshold voltage V_{th}, the charge in the channel of a carbon nanotube field-effect transistor depends linearly on the gate voltage, but the dependence of the conductance is exponential. Thus, the conductance is extremely sensitive to the charge in the channel, and this is the basis for utilizing carbon nanotube field-effect transistors as ultrasensitive sensors. The concept is illustrated in Figure 8.2. Wether the field-effect transistor is *p*-type or *n*-type, addition of negative charge in the channel leads to a shift of the threshold voltage to more negative values, while addition of positive charge leads to a positive threshold voltage shift. The transfer of positive charge to the carbon nanotube is detected with a *p*-type device by working in the OFF state, with the added positive charge causing a turn-on of the device. Similarly, negative charge is detected when a *p*-type

device initially in the ON state turns off upon addition of negative charge to the nanotube. (These are simply reversed for a *n*-type device.) This general mechanism applies regardless of wether the device consists of a single nanotube or a network of nanotubes, as long as it has a clear gating effect.

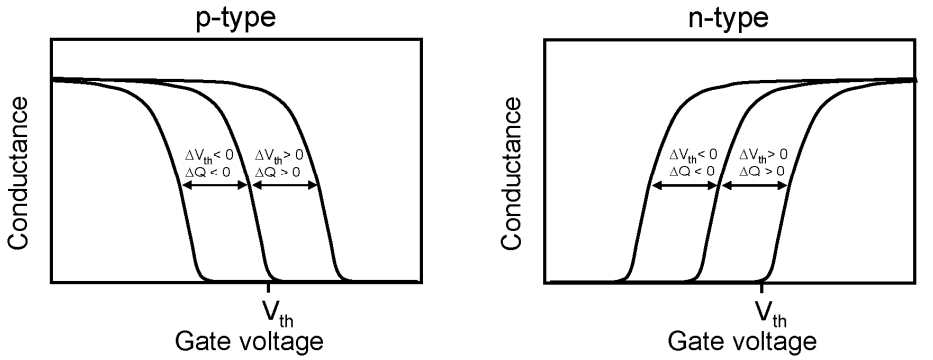

Figure 8.2: Sketch of the impact of charge transfer on the characteristics of carbon nanotube field-effect transistors, for *p*-type and *n*-type devices. ΔV_{th} is the shift of the threshold voltage upon transfer of charge ΔQ to the carbon nanotube.

Near the threshold voltage, the charge in the channel is proportional to the gate voltage according to

$$en = C\left(V_g - V_{th}\right) \tag{2.1}$$

where C is the capacitance per unit length between the gate and the nanotube and n is the number of electrons per unit length. In the presence of analytes on the nanotube surface, this equation is modified to

$$en + e\alpha\theta a^{-1}d = C\left(V_g - V_{th}\right) \tag{2.2}$$

where α is the number of electrons transferred per molecule, a is the area that a molecule occupies on the nanotube surface, d is the nanotube diameter, and θ is the surface coverage. By writing $V_{th} = V_{th}^0 + \Delta V_{th}$ we obtain

$$\Delta V_{th} = e\alpha\theta C^{-1}a^{-1}d. \tag{2.3}$$

The largest change in the nanotube field-effect transistor conductance will occur when the device is operated near the threshold voltage. In this regime, the relative change in conductance is

$$\frac{\Delta G}{G} = S^{-1}\Delta V_{th} = S^{-1}e\alpha\theta C^{-1}a^{-1}d \tag{2.4}$$

where S is the subthreshold swing as discussed in Chapter 4. Using the expression for the capacitance per unit length $C = \dfrac{2\pi\varepsilon}{\ln(4h/d)}$ we can obtain an expression for the maximum relative change in conductance

$$\left(\frac{\Delta G}{G}\right)_{\max} = \frac{e^2 d a^{-1} \ln(4h/d)}{2\pi\varepsilon kT \ln 10} \text{ decades.} \tag{2.5}$$

This expression is valid for complete coverage of the nanotube with analytes, in a device with the mimimum possible subthreshold swing. As an example, for a nanotube of 1 nm diameter with a SiO_2 gate oxide thickness of 100 nm and an analyte occupying a surface area of 1 nm^2, we obtain a maximum ratio of about 75 decades. Of course, this value is unphysically high because the device conductance saturates, but the estimate drives the point that the change in nanotube conductance can be extremely large. At the other end of the spectrum, one can consider the impact of a single analyte on the nanotube conductance. Under the assumption that the transferred charge is delocalized over the entire channel length, we can estimate the relative change in conductance to be

$$\left(\frac{\Delta G}{G}\right)_{\min} = \frac{e^2 \alpha \ln(4h/d)}{2\pi\varepsilon kT \ln 10} \frac{1}{L} \text{ decades.} \tag{2.6}$$

The appearance of the channel length is made explicit in this expression. With the same parameters as above, we estimate a value for the ratio of $\alpha(75\text{ nm}/L)$ decades; for an analyte that transfers a full electron, a change of a factor of two in the conductance requires a channel length of less than 125 nm.

For detection of analytes of concentration c in a gas or liquid phase, it is useful to relate the surface coverage θ to the analyte concentration [Tal06b, Qi06]. This can be accomplished by considering equilibrium surface coverage with analyte binding energy E_b and analyte chemical potential in the gas or liquid μ. The partition function is then given by

$$Z = 1 + z_{vib} e^{-(\mu - E_b)/kT} \tag{2.7}$$

where z_{vib} is the vibrational contribution. The chemical potential can be written as

$$\mu = \mu_0 + kT \ln x \tag{2.8}$$

where x is the mole fraction of the analyte, and μ_0 is the chemical potential of the pure substance. For small mole fractions, the nanotube surface coverage is calculated to be [Bla75]

$$\theta = \frac{c}{c + c_0} \tag{2.9}$$

with

$$c_0 = \bar{c} z_{vib}^{-1} e^{-(\mu_0 - E_b)/kT}. \tag{2.10}$$

The expression for the concentration dependence on the coverage can be combined with that for the threshold voltage shift, Equation (8.3), to obtain

$$\frac{\Delta G}{G} = S^{-1}\Delta V_{th} = e\alpha d S^{-1} C^{-1} a^{-1} \frac{c}{c + c_0}. \qquad (2.11)$$

From this equation and measurements of the threshold voltage shift as a function of the analyte concentration, the amount of charge transfer can be calculated. An example of the application of this approach is shown in Figure 8.3. There, experimental data [Qi03] for the relative conductance change of carbon nanotube network transistors when exposed to NO_2 is plotted as a function of the partial pressure of NO_2. Assuming that the concentration is proportional to the partial pressure, Equation 8.11 can be used to obtain a relatively good description of the experimental data, as the solid line in the figure indicates.

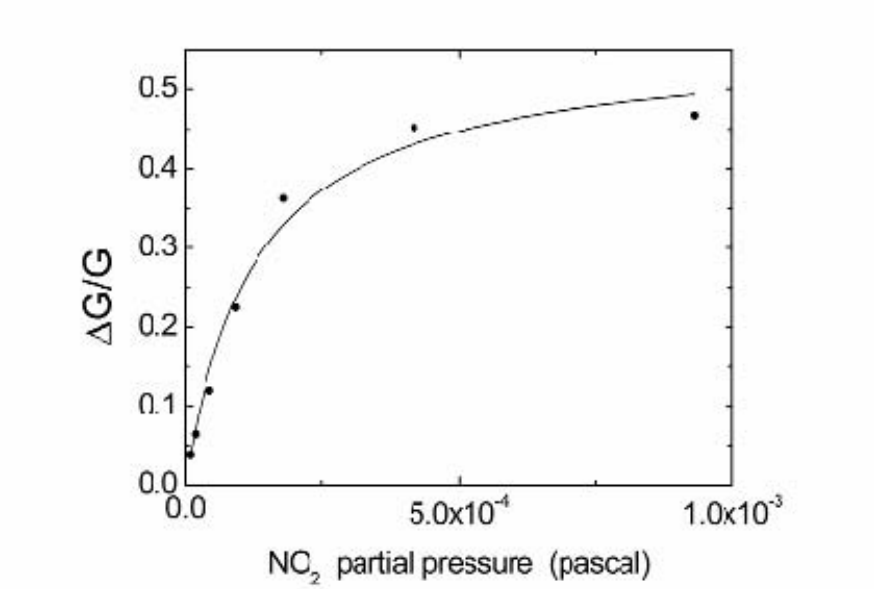

Figure 8.3: Relative conductance change of carbon nanotube transistors when exposed to NO_2. The symbols were extracted from Ref. [Qi03] and the solid line is the best fit using Equation (8.11).

The best fit gives a value for the prefactor $e\alpha S^{-1} C^{-1} a^{-1} d$ equal to 0.56. For this device, the channel is 4 microns long, the oxide is 500 nm thick, and there are 20 to 30 nanotubes in the channel separated by ~4 microns. Using Equation (7.49) with $N = 25$ and assuming a nanotube diameter of 2 nm, we obtain a device capacitance $C = 7.5 \times 10^{-10}$ F/m. From the device transfer characteristics, a subthreshold swing of $S = 14.2$ V/decade can be extracted, and for a molecular size $a = 10^{-19}$ m^2 a charge transfer of 0.07 electrons per molecule is obtained.

One of the early experiments that supported the charge transfer model consisted in measuring the resistance of networks of carbon nanotubes in vaccum and in oxygen-rich environments. The time-dependence of the resistance during such an exposure to air is shown in Figure 8.4, where one can see that the resistance of the nanotube network decreases in air, with a full recovery observed as the device is returned to ultrahigh

vacuum conditions. Based on the above discussion, the reduction in the resistance could arise from charge transfer if the nanotubes are *n*-type in vacuum and positive charge is transferred to them, or if the nanotubes are *p*-type and negative charge is transferred. While the simplest way to distinguish between these two possibilities is to sweep the gate volgate and obtain the transfer characteristics, a complementary method is to measure the Seebeck coefficient *S*. In thermoelectric materials, the Seebeck coefficient, defined as $s = dV / dT$, is a measure of the voltage generated across the material when a temperature difference is applied across it. The sign of *s* depends on the type of charge carrier: for a *p*-type (*n*-type) material *s* is positive (negative). Thus, concomitant measurements of the resistance and the Seebeck coefficient can provide evidence for the type of doping in the carbon nanotubes. Figure 8.4 shows the measured Seebeck coefficient for a nanotube network device, indicating that in vacuum, the nanotubes are *n*-type, but that exposure to oxygen gives *p*-type doping. The implication is that oxygen transfers positive charge to the carbon nanotubes.

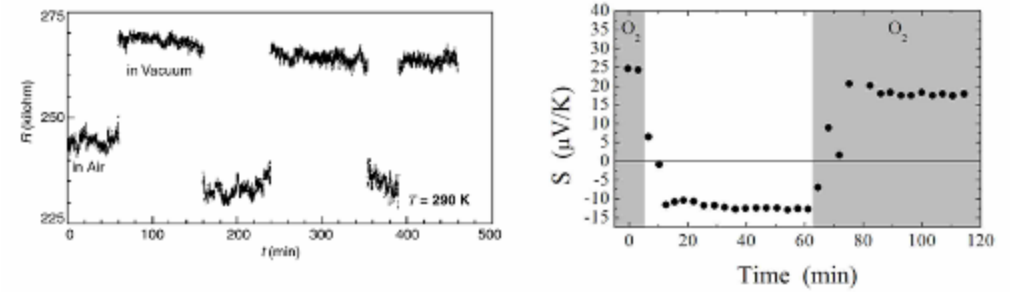

Figure 8.4: Measured resistance (left, *from Ref. [Col00]*) and Seebeck coefficient (right, *after Ref. [Col00]*) of carbon nanotube films in vacuum and when exposed to air.

First principles calculations have been performed to study the properties of single carbon nanotubes with oxygen adsorbates [Gru03, Tch06]. The central result of these calculations is that oxygen molecules bind weekly to pristine zigzag and armchair nanotubes, wether they are semiconducting or metallic. The calculated binding energies for these situations are on the order of 0.05 eV, indicating physisorption on the nanotube wall. Furthermore, it is found that charge transfer from the nanotube to the oxygen molecule is weak, on the order of 0.01 electrons. The same calculations have found, however, that defects in the carbon nanotube lattice can have a profound effect on oxygen absorption. For example [Gru03], the binding energy of an oxygen molecule to a so-called 7-5-5-7 defect is on the order of 0.3 eV, with 0.4 electrons transferred from the nanotube to the oxygen molecule. As will be discussed in a later section, experiments have suggested that oxygen may have a profound impact on the properties of the nanotube/metal contacts [Der02], which may dominate the sensor response.

The shift in the threshold voltage of carbon nanotube transistors when exposed to analytes has been observed in a number of experiments. Support for the charge transfer model can be obtained by studying analytes with differing electron donating properties [Sta03a]. For example, monosubstituted benzenes such as aniline, phenol, toluene, chlorobenze, and nitrobenzene are believed to bind non-covalently to carbon nanotubes, but posses much different electron donating properties. A measure of this property is the

Hammett parameter σ_p, which was introduced by Hammett [Ham37] to describe the relationship between reaction rates and equilibrium properties of organic reactions. This parameter is related to the electron donating or withdrawing properties of the substituents on the benzene ring. The parameter is defined as zero for benzene, is positive for electron withdrawing species, and negative for electron donating species.

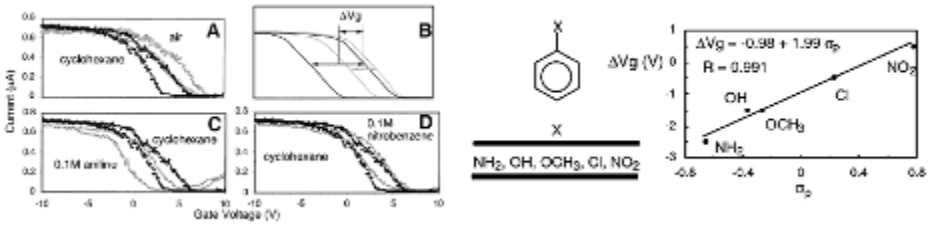

Figure 8.5: Left: Impact of aromatic compounds on the transfer characteristics of carbon nanotube network transistors. Panel B shows the definition of the threshold voltage shift taking into account hysterisis. Middle: The monosubstituted aromatic compounds studied. Right: Measured threshold voltage shift of carbon nanotube field-effect transistors when exposed to aromatic compounds as a function of their Hammet parameter σ_p. *Figures from Ref. [Sta03a].*

Figure 8.5 shows the transfer characteristics of carbon nanotube network transistors when exposed to solutions of cyclohexane, and solutions of cyclohexane with 0.1M aniline and nitrobenzene. (The conductivity of these liquids is low, and the device conductance is dominated by the carbon nanotube.) The general behavior is for the transfer characteristics to be shifted to the left or right, with the conductance in the ON state unaffected by the presence of the aromatic compounds. This behavior suggests that the analytes do not cause additional scattering in the carbon nanotube, while possibly causing a charge transfer that shifts the transfer characteristics. The devices show hysterisis; an average threshod voltage shift can be calculated using the procedure depicted in Figure 8.5. From this procedure, the threshold voltage shift is found to depend linearly on the Hammett parameter of the different substituents, as shown in Figure 8.5.

Charge transfer effects can also arise when the workfunction of metal clusters on carbon nanotubes is modified by analytes [Kon01b]. For example, it is well-known that hydrogen diffuses readily into palladium, which can lead to a change in its workfunction. Indeed, this mechanism forms the basis of hydrogen gas sensor technologies. It is possible to take advantage of this mechanism in carbon nanotube devices by decorating the nanotube surface with nanoparticles of Pd. This is accomplished by first assembling a carbon nanotube electronic device, followed by electron beam evaporation of Pd on the whole device, leading to Pd nanoparticles decorating the nanotube sidewalls (Figure 8.6). (The nanoparticle layer is not continuous, and the electronic transport is through the nanotube.)

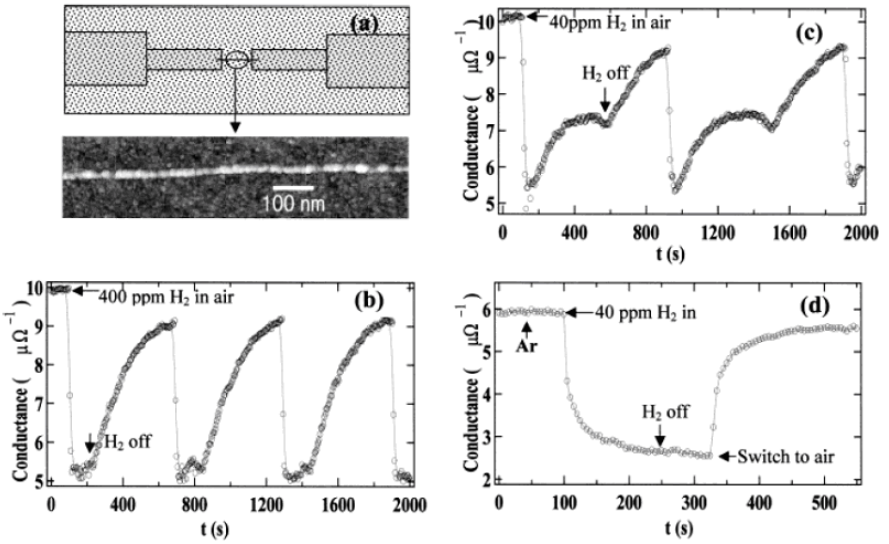

Figure 8.6: Upper left: Schematic of the nanotube device with Pd nanoparticles coating the nanotube. Middle left: Atomic force microscopy image of an individual carbon nanotube decorated with Pd nanoparticles of diameters ranging from 2 nm to 3.5 nm. (b) Conductance of nanotube device when exposed to 400 ppm of hydrogen in air. (c) Conductance of nanotube device when exposed to 40 ppm of hydrogen in air. (d) Conductance of nanotube device when exposed to 40 ppm of hydrogen in Ar, and them switched to air. *Figure from Ref. [Kon01b].*

The conductance of the Pd-decorated nanotube device decreases substantially when it is exposed to 400 parts-per-million of hydrogen in an air flow (Figure 8.6b), with a response time on the order of 5 to 10 seconds. Device recovery upon turn-off of the hydrogen gas is complete and occurs on a time scale of 400 seconds. It is believed [Kon01] that the sensing mechanism is electron transfer from the Pd nanoparticles to the carbon nanotube due to a lowering of the Pd workfunction, which reduces the hole carrier concentration and decreases the conductance. It is interesting to note that competing hydrogen reactions can lead to an overshoot of the conductance reduction at low hydrogen concentrations. For example, Fig, 8.6c shows that for 40 parts-per-million of hydrogen in air, the initial large drop of the conductance on the 5 to 10 second timescale is followed by a partial recovery of the conductance while the hydrogen is still flowing in the chamber. Experiments with the same concentration of hydrogen in Ar show that this behavior is not present, but that switching to air gives a full device recovery (Figure 8.6d). A likely scenario is that the hydrogen dissolved in the Pd reacts with oxygen in air, causing the hydrogen to leave the Pd in the form of water.

8.1.2 Scattering

The impact of analytes on the conductance of carbon nanotubes can also occur through an increased scattering of electrons in the channel. In this case, and in the absence of charge transfer and contact effects, the transfer characteristics of carbon nanotube transistors are expected to be modified according to Figure 8.7. The figure shows that the threshold

voltage is unaffected by the analytes, but that the ON state conductance, and hence the subthreshold swing, is reduced because of increased scattering.

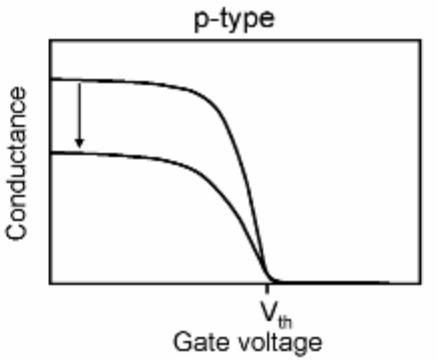

Figure 8.7: Illustration of the impact of increased scattering on the transfer characteristics of a *p*-type carbon nanotube field-effect transistors. The threshold voltage is unchanged, but the conductance in the ON state and the subthreshold swing decrease.

The simplest model to describe the impact of analytes on the nanotube conductance is one where each analyte is treated as a point scatterer for coherent carrier scattering. In Equation (4.102) and Figure 4.47, we considered the transmission probability for an electron in the presence of two scatterers in series. Generalization to N scatterers in series each with transmission probability T_0 gives the expression for the total transmission probability

$$T = \frac{T_0}{T_0 + N\left(1 - T_0\right)}. \tag{2.12}$$

For a single scatterer $(N = 1)$ the total transmission $T = T_0$ while in the limit of large N such that $N \gg \frac{T_0}{1 - T_0}$ we have $T \sim \frac{1}{N}\frac{T_0}{1 - T_0}$. This last expression is also valid at any N (including $N = 1$) if the transmission probability of an individual scatterer is small.

The time-dependence of the conductivity can be obtained by considering the number of analytes on the surface of the nanotube as a function of time. For analytes that attach to the surface of the nanotube with probability λ, the number of analytes depends on time as

$$N(t) = \frac{Ld}{a}\left(1 - e^{-\lambda \Phi a t}\right) \tag{2.13}$$

where Φ is the number of analytes impinging on the nanotube per unit time per unit area, a is the area that the analyte occupies on the surface of the nanotube, L is the length of the nanotube, and d its diameter. The ratio Ld/a, representing the maximum number of analytes that can attach on the surface, is somewhat approximate, but reflects the fact that nanotubes typically sit on a substrate, so only a portion of the nanotube surface is available for attachment. Combining Equations (8.1) and (8.2) with the Landauer expression for the conductance G [Equation (2.11) at zero temperature for a single, degenerate transmission channel], we obtain the time-dependent conductance as

$$G(t) = \frac{4e^2}{h} \frac{T_0}{T_0 + \frac{Ld}{a}(1-T_0)\left(1-e^{-\lambda \Phi at}\right)}. \qquad (2.14)$$

By fitting to experimental data, this formula can be utilized to extract the transmission coefficient of a single scatterer T_0 as well as the sticking probability λ.

More detailed theoretical work has been performed to understand the role of analytes on nanotube conductance [Lat05]. For example, the impact of benzene (C_6H_6) and azulene $(C_{10}H_8)$ on the nanotube electronic structure and electronic transport has been studied by calculating the distortions of the nanotube electronic structure in the presence of analytes, mapping this distortion into a tight-binding parametrization, and calculating the scattering mean-free path. It is found that these simple molecules do not disturb the nanotube electronic structure significantly, especially around the Fermi level. Thus the scattering mean-free paths are found to be larger than 7 microns for azulene, and larger than 100 microns for benzene even at coverages up to 20% by mass. This indicates that surface functionalization of carbon nanotubes with molecules through π-stacking interactions will not appreciably distort the electronic structure or the transport properties. It also indicates that sensing through monitoring of the ON state conductance is more effective with molecules that chemisorb on the nanotube surface rather than physisorbed species like aromatic hydrocarbons.

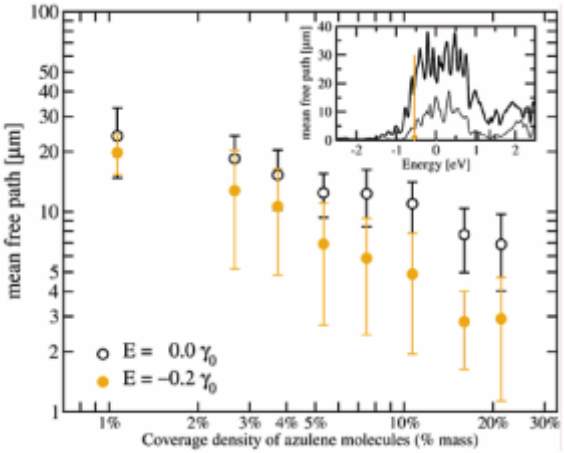

Figure 8.8: Calculated mean-free path for electron scattering with physisorbed azule molecules. At the Fermi level (open circles), the mean-free path is longer than 7 microns, even at the highest coverages. *Figure from [Lat05].*

8.1.3 Contacts

As we have seen in previous chapters, contacts play an important role in carbon nanotube devices. In particular, the band alignment at nanotube/metal contacts depends strongly on the metal workfunction. Thus, analytes can have a serious impact on the conductance of nanotube devices if they modify the metal workfunction at the contact. Experiments

using Kelvin probes have shown that the band alignment at nanotube/Au interfaces can be changed by as much as 0.1 eV upon exposure to oxygen [Cui03].

Initial evidence for the importance of contacts in carbon nanotube sensors was provided by the study of single-nanotube field-effect transistors with Au contacts first annealed in vacuum and then exposed to various doses of oxygen [Der02]. Contrary to as-prepared devices, annealing the devices in vacuum leads to *n*-type field-effect transistors, as we have discussed in the context of logic circuits in Chapter 4. Exposure of these devices to oxygen leads to a recovery of the *p*-type behavior, as illustrated in Figure 8.9. Importantly, it is found that the threshold voltage of the nanotube transistor is essentially unaffected by the presence of oxygen; instead, a gradual reduction of the conductance for positive voltages and a gradual increase of the conduction for negative gate voltages is observed. This behavior indicates modification of the Schottky barriers at the contacts. As the sketches of Figure 8.9 illustrate, a device in vacuum initially has a metal Fermi level aligned close to the conduction band edge, leading to *n*-type behavior. As the oxygen dosage is increased, the Au Fermi level moves deeper into the bandgap, leading to ambipolar behavior. Finally, at the highest oxygen dosage, the Schottky barrier for holes is smaller than that for electrons, and the device behaves as a *p*-type transistor.

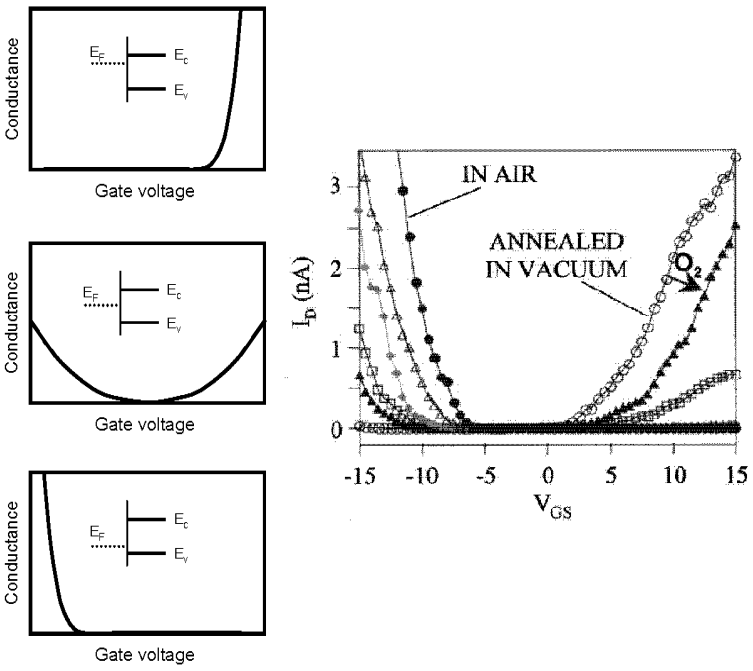

Figure 8.9: Left: Sketch of the impact of a change in metal workfunction due to analytes on the transfer characteristics of carbon nanotube transistors. Right: Measured transfer characteristics in vacuum and at different doses of oxygen, indicating a gradual change from *n*-type to *p*-type behavior. *Right figure from Ref. [Der02].*

To further explore the role of contacts, recent experiments have looked at the sensing properties of carbon nanotube transistors with contacts protected by polymeric layers

[Zha06] or self-assambled monolayers [Che04]. Figure 8.10 shows the transfer characteristics of a carbon nanotube transistor with unprotected top Pd contacts of 75 nm thickness upon exposure to NO_2. In this experiment, the concentration of NO_2 in the chamber depends on time according to $n(t) = n_0\left(1 - e^{-t/t_0}\right)$ where $t_0 = 23$ min. Measurement of the transfer characteristics of the nanotube transistor shows that the current in the ON state increases with exposure time, and can be as much as a factor of three larger than for the device before exposure. A comparison of the time dependence of the conductance shows that it correlates with the time dependence of the NO_2 concentration in the chamber (Figure 8.10). Similar experiments with a SU-8/PMMA polymeric protective layer of 2 micron thickness over the contacts (but leaving the nanotube channel unprotected) gives a different result: it is found that the time dependence of the conductance no longer correlates with the time dependence of the NO_2 concentration in the chamber, but instead varies much more slowly with time.

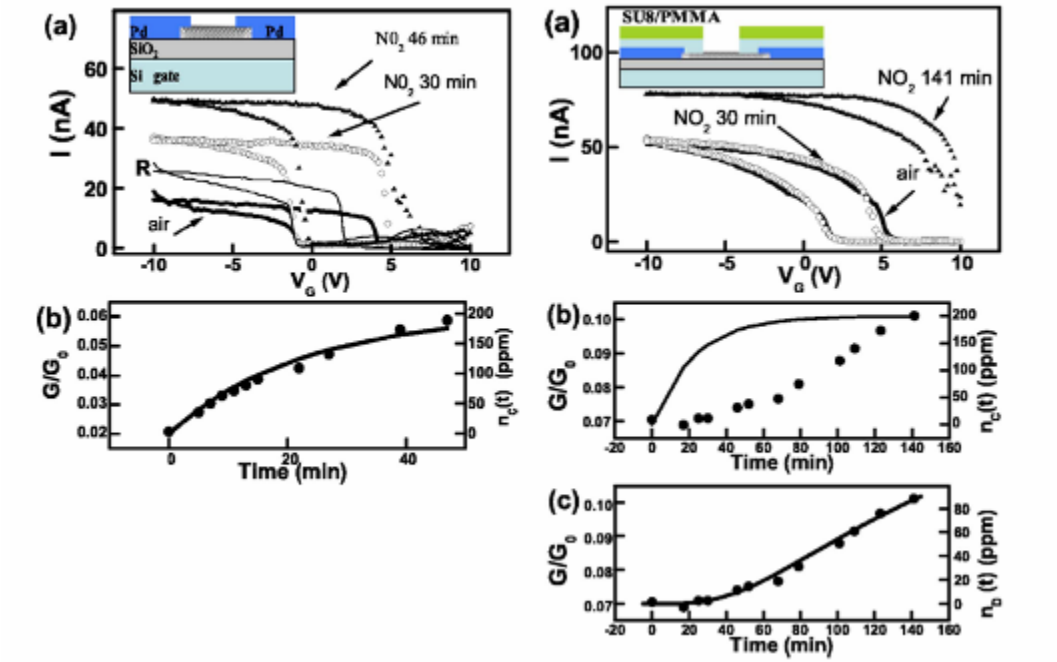

Figure 8.10: Transfer characteristics of a carbon nanotube field-effect transistor upon exposure to NO_2. The left and right panels show the results without and with a SU-8/PMMA protective layer on the contacts. The panels labeled (b) in both figures compare the measured time-dependence of the conductance with the expected time dependence of the concentration inside the chamber (solid line). The bottom right panel shows a comparison of the measured conductance with the calculated concentration of NO_2 from diffusion across the SU-8/PMMA layer. *Figures from Ref. [Zha06].*

This observation can be explained by considering the concentration of NO_2 that diffuses through the protective layer and reaches the metal/nanotube interface. The situation is illustrated in Figure 8.11. There, a protective layer of thickness L sits on top of a carbon nanotube. At the outer surface, exposed to the chamber, there is a time-dependent concentration of NO_2 given given by that in the chamber. The time dependence of the concentration throughout the layer is obtained by solving the diffusion equation for the concentration

$$\frac{\partial c(x,t)}{\partial t} = D\frac{\partial^2 c(x,t)}{\partial x^2} \tag{2.15}$$

with the boundary condition at the surface

$$c(0,t) = c_0\left(1 - e^{-t/t_0}\right) \tag{2.16}$$

which corresponds to the concentration in the chamber. We assume that there is no flux of NO_2 through the bottom surface of the polymer layer, so that the boundary condition there is

$$\left.\frac{\partial c}{\partial x}\right|_{x=L} = 0. \tag{2.17}$$

The initial condition is $n(x,0) = 0$. The diffusion equation in the presence of time-dependent boundary conditions can be solved with the change of variables

$$u(x,t) = c(x,t) - c_0\left(1 - e^{-t/t_0}\right) \tag{2.18}$$

leading to the non-homogeneous differential equation

$$\frac{\partial u(x,t)}{\partial t} - D\frac{\partial^2 u(x,t)}{\partial x^2} = \frac{c_0}{t_0}e^{-t/t_0} \tag{2.19}$$

with the boundary conditions $u(0,t) = 0$ and $\partial_x u(L,t) = 0$. The original differential equation has been transformed to a non-homogeneous differential equation but with homogeneous boundary conditions. The solution of this equation can be obtained by following standard procedures [Boy86], leading to the full solution for the concentration:

$$c(x,t) = c_0\left(1 - e^{-t/t_0}\right) - c_0\sum_{m=1,3,5,\ldots}^{\infty}\frac{2}{\pi m}\frac{e^{-t/t_0} - e^{-\frac{D\pi^2 m^2}{4L^2}t}}{\frac{D\pi^2 m^2}{4L^2}t_0 - 1}\sin\left(\frac{\pi m}{2L}x\right). \tag{2.20}$$

Figure 8.11 shows the time evolution of the concentration profile for a film thickness of 2 microns, a diffusion constant $D = 1.8\times10^{-16}$ m^2/s, and $t_0 = 23$ min. Because the diffusion constant leads to a characteristic diffusion time $\sqrt{L/D} \approx 1500$ min much longer than the time necessary to achieve the steady-state concentration in the chamber, the concentration at the nanotube/metal interface lags behind that in the chamber, and is typically about 50% less for the parameters used here. The calculated concentration at the nanotube/metal interface correlates well with the time dependence of the conductance as shown in Figure 8.10c. Furthermore, experiments where the whole device was covered in SU-8/PMMA showed the same behavior as the devices where only the contacts were protected, providing further evidence that for NO_2 the sensing mechanism is due to changes in the contact properties.

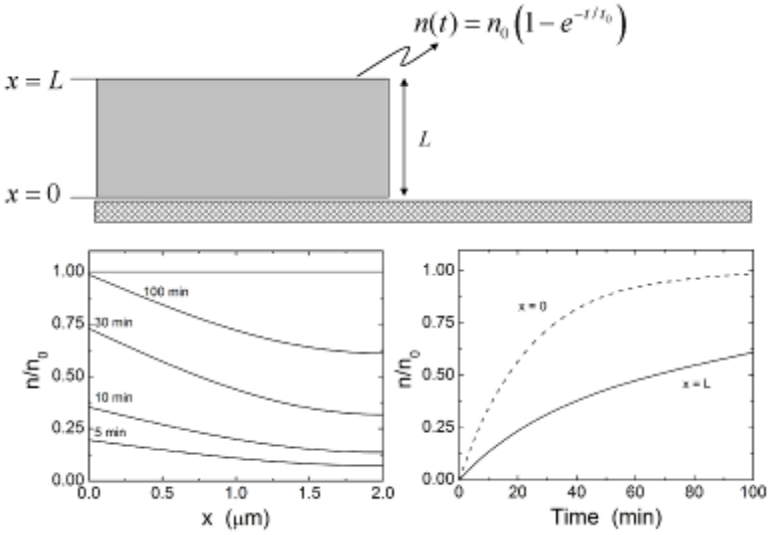

Figure 8.11: Top: Schematic of the protective layer sitting on top of a carbon nanotube. Bottom left: Calculated concentration profile for diffusion through a 2 micron thick layer, with a time-dependent boundary condition at the surface exposed to the chamber. Because of the finite diffusion coefficient, the concentration at the unexposed end of the layer $(x = L)$ lags behind the concentration at the surface. Bottom right: Calculated time dependence of the concentration at the nanotube surface (solid line) compared to that at the exposed surface (dashed line).

The change in the transfer characteristics due to diffusion of NO_2 to the nanotube/metal interface is most likely due to a decrease of the Schottky barrier. This is consistent with the increase of the ON state conductance with increased exposure. An alternative mechanism that could also apply to sensors with metallic carbon nanotubes arises if there is a tunneling barrier at the nanotube/metal interface. In this case, the presence of analytes can change the height of the tunneling barrier, causing an increase or decrease of the conductance. To explore this possibility, we consider tunneling across a thin vacuum layer at the interface between the metallic carbon nanotube and the metal contact, forming a metal/insulator/metal device, as illustrated in Figure 8.12.

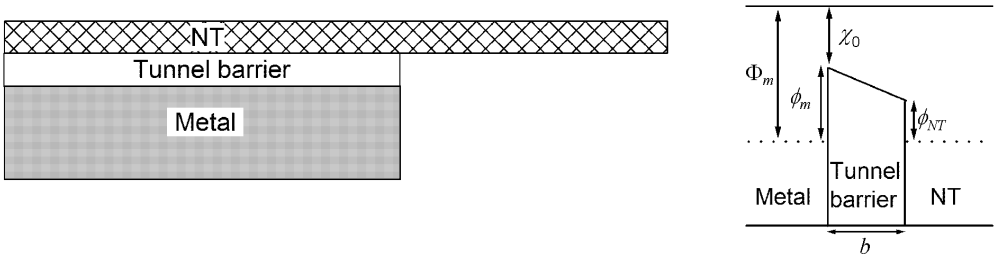

Figure 8.12: Illustration of a metal/metallic-nanotube interface with a thin tunneling barrier, and the band alignment defining the thickness of the tunnel layer b, the tunnel barrier heights on the metal ϕ_m and nanotube sides ϕ_{NT}, the metal workfunction Φ_m and tunnel barrier electron affinity χ_0.

The tunneling current in such a system is given by [Sze81]

$$I = I_0\left[\left(\phi - V/2\right)\exp\left(-\sqrt{\phi - V/2}/V^*\right) - \left(\phi + V/2\right)\exp\left(-A\sqrt{\phi + V/2}/V^*\right)\right] \quad (2.21)$$

where ϕ is the height of the tunnel barrier, and

$$V^* = \frac{\hbar}{eb}\sqrt{\frac{\phi}{m*}}. \quad (2.22)$$

In this last equation $m*$ is the effective mass of the tunneling electrons, and b is the tunneling distance. For simplicity we assume that $\phi = \left(\phi_{NT} + \phi_m\right)/2$ where ϕ_{NT} is the height of the tunnel barrier on the nanotube side, and ϕ_m is the height of the tunnel barrier on the metal side. For small bias voltages, the current depends on the barrier height as

$$I = \tilde{I}\exp\left(-\frac{2b\sqrt{2m*}\sqrt{\phi}}{\hbar}\right) \quad (2.23)$$

where the voltage dependence has been included in the prefactor $\tilde{I}$. We assume that the height of the tunnel barrier depends linearly on the concentration of analyte at the contact (for example, through a change in the metal workunction). For an unprotected contact, or for fast diffusion of the analyte through the protective layer, we have

$$\phi(t) = \phi_0 + \Delta\phi\left(1 - e^{-\lambda\Phi Ldt}\right) \quad (2.24)$$

where $\Delta\phi$ is the change in barrier height with concentration, λ is the sticking coefficient, Ld is the nanotube area available to analytes, and Φ is the flux of analytes on the nanotube surface. This sensing mechanism therefore gives a unique signature in the time-dependence of the conductance which allows to distinguish it from other mechanisms.

8.1.4 Capacitance

While this chapter has focused mainly on changes of the nanotube conductance due to analytes, an alternative approach to detect the presence of analytes is through the measurement of the capacitance. This approach has so far been demonstrated using networks of carbon nanotubes, and applied to sensing of various chemical species and agents [Sno05, Ese07]. Figure 8.13 illustrates a device utilized to perform these measurements. It consists of a network of carbon nanotubes, with a mixture of semiconducting and metallic nanotubes. An interdigitated array of Pd electrodes is patterned on top of the nanotube network, which sits on SiO_2. An AC voltage is applied between the nanotube network (through the Pd electrodes) and a backgate, and the capacitance is measured by detecting the out-of-phase AC current with a lock-in amplifier. Figure 8.13 shows the results of such capacitance measurements when the nanotube network is exposed to dimethyl formamide of varying vapor concentrations. The figure clearly indicates a noticeable change in the capacitance on a short time scale, both for the turn-on and the recovery (the response time is less than 4 seconds, limited by the vapor-delivery system). A broad range of analytes have been shown to give a capacitance response, and notably, a minimum detectable level of 50 parts per billion has

been achieved for dimethylmethylphosphonate (DMMP), a chemical used in the synthesis of the nerve agent sarin [Sno05]. Comparisons with commercial chemicapacitors are quite favorable. For example, commercial chemicapacitors can detect acetone with a minimum detection limit of 2 parts-per-million and detection time of 228 seconds. This can be compared with the values of 0.5 parts-per-million and detection time of less thatn 4 seconds for the nanotube network capacitor. Similar conmparisons for the detection of DMMP are equally favorable.

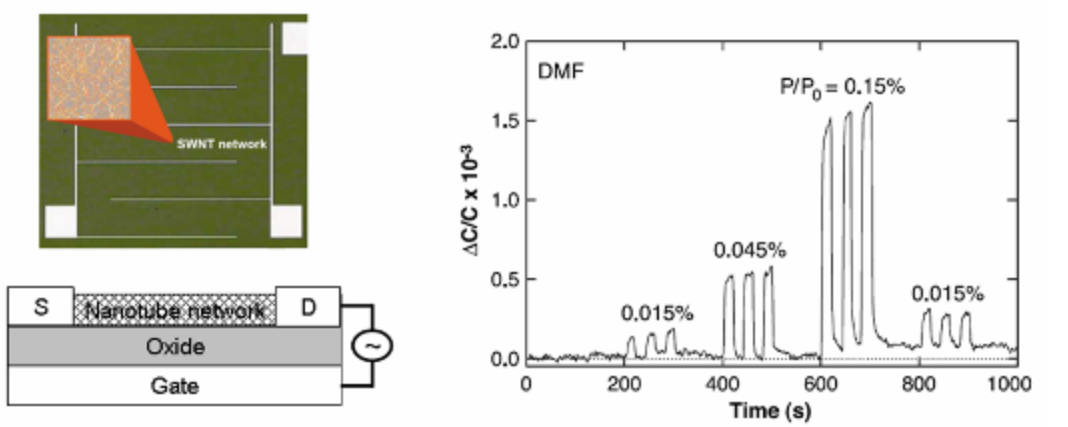

Figure 8.13: Left: Optical micrograph and cross-sectional sketch of a carbon nanotube network capacitor used for sensing experiments. The capacitance is measured by applying an AC voltage between the nanotube film and the gate. Right: Relative change in capacitance when the device is exposed to dimethyl formamide (DMF). *Figures from Ref. [Sno05].*

It has been proposed that the change in capacitance is due to the dipole moments of the analytes, which can change the effective dielectric constant of the capacitor [Sno05]. While some polar molecules have shown increased capacitance sensitivity compared to non-polar molecules, measurements across a broad range of molecular dipole moments do not show a strong correlation. This has lead to controlled experiments [Ese07] to further explore the sensing mechanism in these types of measuments, as we now discuss.

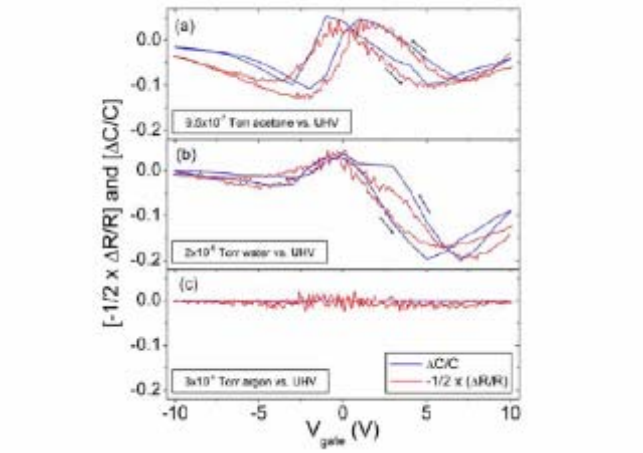

Figure 8.14: Comparison of the measured relative changes in capacitance and resistance for carbon nanotube networks exposed to acetone, water and argon. *Figure from Ref. [Ese07].*

The proposed concept is that the nanotube network device (channel width *w* and channel thickness *t*) behaves like a transmission line with resistance per length *r*, back-gate electrostatic capacitance $c_c = \varepsilon w / t$, inductance $l = \mu_0 t$, and oxide conductance *g*. The impedance of such a transmission line is given by

$$Z = \sqrt{\frac{r + i\omega l}{g + i\omega c_c}}. \tag{2.25}$$

Assuming that the oxide conductance and nanotube network inductance are negligeable, (at frequencies $\omega \ll r / l$) the nanotube network device can be modeled as a transmission line with a characteristic length

$$l_0 = \sqrt{\frac{2}{r\omega c_{el}}}. \tag{2.26}$$

For channel lengths much larger than this characteristic length scale, the impedance is

$$Z = \frac{(1-i)}{\sqrt{2}} \sqrt{\frac{r}{\omega c_{el}}}. \tag{2.27}$$

This can be compared with the impedance of a RC circuit

$$Z = R_{NT} - \frac{i}{\omega C_{NT}}, \tag{2.28}$$

to obtain the effective capacitance of the nanotube network as

$$C_{NT} = \sqrt{\frac{2c_{el}}{\omega r}} = c_{el} l_0. \tag{2.29}$$

Note that this equation indicates that there is an intimate connection between the resistivity of the nanotube network and its capacitance, $C_{NT} \sim r^{-1/2}$. Because of this relationship, the relative sensitivies of the capacitance and the resistance to analytes follows a relation

$$\frac{\Delta C}{C} = -\frac{1}{2}\frac{\Delta r}{r}. \tag{2.30}$$

This equation indicates that the relative change in capacitance can be entirely due to a relative change in the resistivity of the nanotube network. This relationship is confirmed by measurements comparing the capacitance and resistivity changes of carbon nanotube networks in ultra-high vacuum and upon exposure to acetone, water, and argon. As shown in Figure 8.14, in all of these cases the relationship (8.30) is satisfied, indicating that resistivity changes are the most likely mechanism for sensing of these analytes. While the ratio of -1/2 has also been seen by other researchers [Sno07], deviations from this relation also occur [Sno07].

8.1.5 Liquid Gating

"Liquid gating" is not a sensing mechanism per se, but is a technique to achieve strong field-effect behavior in carbon nanotubes when the nanotube is immersed in solution. This is important because many sensing applications require the ability to detect analytes or to monitor reactions occuring in the liquid phase. In this section, we derive an expression for the capacitance of an electrolyte-gated carbon nanotube by adapting the Gouy-Chapman theory of the double-layer capacitance.

The system under consideration is illustrated in Figure 8.15. There, a carbon nanotube of radius R with linear charge density λ is immersed in a charge-neutral electrolyte, and a reference electrode sets the potential at V_{lg} where the subscrip "lg" stands for "liquid gate". For simplicity, we will assume that the reference potential is set infinitely far from the nanotube surface. In the electrolyte, Poisson's equation is

$$\frac{\partial^2 V}{\partial r^2}+\frac{1}{r}\frac{\partial V}{\partial r}=-\frac{\rho(r)}{\varepsilon} \tag{2.31}$$

where $\rho(r)$ is the charge distribution in the electrolyte, and ε is the dielectric constant of the electrolyte.

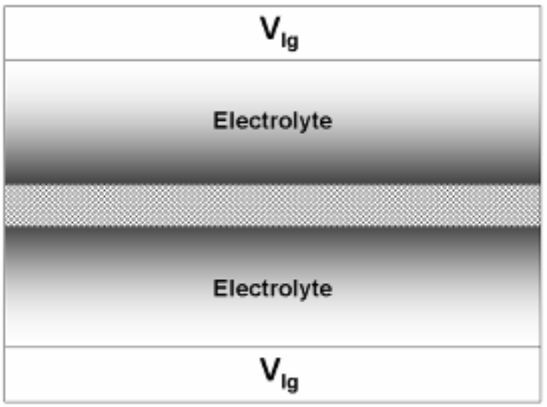

Figure 8.15: Cross-section of the system for calculation of the capacitance of a liquid gate. A carbon nanotube is immersed in an electrolyte, and a reference potential V_{lg} is set far from the nanotube. The grey shading represents the distribution of charge in the electrolyte that screens the charge on the nanotube.

In the Gouy-Chapman theory, it is assumed that the excess concentration $c(r)$ of ions in the solution is given by a Boltzman distribution

$$c(r)=c_0-c_0\exp\left[-\frac{E(r)}{kT}\right] \tag{2.32}$$

where c_0 is the concentration in the neutral solution and $E(r)$ is the energy required to bring an ion from the reference potential to position *r*. In our case that energy for an ion of valence *z* is simply $E(r) = ze\delta V(r)$ and we have

$$c(r) = c_0 - c_0 \exp\left[-\frac{ze\delta V(r)}{kT}\right] \approx \frac{ze\delta V(r)}{kT} \tag{2.33}$$

where the last approximation assumes that the potential is small. Using the relation $\rho(r) = -ezn_0 c(r)$ with n_0 the number of ions per unit volume, we obtain Poisson's equation as

$$\frac{\partial^2 \delta V}{\partial r^2} + \frac{1}{r}\frac{\partial \delta V}{\partial r} = \frac{z^2 e^2 n_0}{\varepsilon kT}\delta V(r). \tag{2.34}$$

The solution of this equation with the boundary conditions that $V = V_{\text{lg}}$ as $r \to \infty$ and $V = 0$ at $r = R$ is

$$V(r) = V_{\text{lg}}\left[1 - \frac{K_0(r/l)}{K_0(R/l)}\right] \tag{2.35}$$

where $K_0(x)$ is the modified Bessel function of order 0. The parameter

$$l = \sqrt{\frac{\varepsilon kT}{z^2 e^2 n_0}} \tag{2.36}$$

has units of length and represents the screening length in the electrolyte. Indeed, for $r \gg l$ the potential can be approximated as

$$V(r) \approx V_{\text{lg}}\left[1 - \frac{1}{K_0(R/l)}\sqrt{\frac{\pi l}{2r}}e^{-r/l}\right] \tag{2.37}$$

so the potential decays over a distance *l*.

To obtain the capacitance we calculate the charge induced on the nanotube from

$$Q_{tot} = \frac{2\pi z^2 e^2 n_0 V_{\text{lg}} L}{kT}\int_R^\infty \frac{K_0(r/l)}{K_0(R/l)} r dr \approx \frac{2\pi\varepsilon V_{\text{lg}} L}{K_0(R/l)} \tag{2.38}$$

where *L* is the nanotube length. The capacitance per unit length is then

$$\frac{C_{\text{lg}}}{L} = \frac{2\pi\varepsilon V_{\text{lg}}}{K_0(R/l)} \approx \frac{2\pi\varepsilon}{\ln(2l/R\gamma)}. \tag{2.39}$$

In this last equation γ is Euler's constant and we assumed that $R \ll l$. This expression for the capacitance can be compared with that of a backgate

$$\frac{C_{bg}}{L} = \frac{2\pi\varepsilon}{\ln(2h/R)}. \tag{2.40}$$

While both have the same functional form, there are two crucial differences. First, the dielectric constant of electrolytes is typically much larger than that of gate insulators (water has a dielectric constant of 80 for example). Second, the gate-oxide thickness is replaced with the length scale $2l/\gamma$ and for water this is on the order of 1 nm. The combination of these two factors leads to a liquid-gate capacitance per unit length on the order of 10 aF/nm, two orders of magnitude larger than a typical backgate capacitance. An important implication of this result is that the intrinsic capacitance of the nanotube, which is usually neglected because it is much larger than the backgate capacitance, becomes the dominant capacitance. As will be discussed below, liquid-gating has been utilized to detect protein binding [Che03] and enzymatic reactions[Bes03].

8.2 Functionalized Nanotubes

From the discussion in the previous sections, it is quite clear that carbon nanotubes are quite sensitive to their environment. While this can be advantageous for sensing applications, the extreme sensitivity to the environment also implies that analyte specificity is more difficult to achieve. To this end, functionalization of the nanotube surface has been explored to target specific chemical and biological agents. The functionalization schemes fall into two classes: selective schemes where the functionalization reacts only with a limited range of analytes, and blocking schemes where a surface layer allows only a few analytes to reach the carbon nanotube.

8.2.1 DNA Functionalization

Single-stranded DNA (ssDNA) was initially utilized in the carbon nanotube arena as a surfactant to isolate individual nanotubes in solution [Zhe03]. Electrical measurements subsequently showed that the ssDNA does not alter the conductance of individual nanotubes appreciably [Tal04]. Because of this preservation of the high nanotube conductance and the unique recognition capability of ssDNA, sensors with ssDNA-functionalized carbon nanotubes have been explored [Sta05, Sta06, Tan06].

In one example [Sta05], a carbon nanotube field-effect transistor made of a single carbon nanotube is fabricated, with ssDNA applied to the carbon nanotube by deposition of a drop of distilled water with diluted ssDNA. Two different sequences of ssDNA were applied to the carbon nanotube: a 21-mer sequence (5’ GAG TCT GTG GAG GAG GTA GTC 3’, sequence 1) and a 24-mer sequence (5’ CTT CTG TCT TGA TGT TTG TCA AAC 3’, sequence 2). These sequences are chosen because previous experiments in the context of artificial noses demonstrated their sensitivity to small, vapor-phase molecules. Atomic force microscopy of the same nanotube before and after application of the ssDNA solution indicates an increase in the apparent height from 5.4 m. to 7.2 nm, indicating the presence of a 1-2 nm thick layer of ssDNA on the surface of the nanotube. Support for the formation of ssDNA/carbon nanotube hybrids has also been provided by

other experiments where the nanotubes were functionalized with ssDNA in solution, with subsequent heating of the solution above 80 ^{0}C leading to precipitation of the carbon nanotubes, indicating dissociation of ssDNA from nanotube surface [Tal04].

The mild effects of ssDNA sequence 1 on the conductance of carbon nanotubes is illustrated in Figure 8.16, which plots the measured transfer characteristics of the nanotube device before and after functionalization. A small reduction in the ON state conductance is observed, accompanied by a shift of the threshold voltage from 10 V to 5 V. The threshold voltage shift may be an indication that ssDNA of this sequence transfers electrons to the carbon nanotube. Exposure of the ssDNA/nanotube hybrid device to trimethylamine (TMA) by flowing a mixture of air/analyte over the device shows a very strong shift of the threshold voltage by about 10 V. We note however that the bare carbon nanotube also shows a response to TMA, although as discussed further below, the response is not as strong. Since TMA has a large pK value of 9.8, it is proposed that TMA is protonated by residual water. This would be consistent with the presence of residual water on bare nanotubes, and is also expected after exposure to the ssDNA diluted in distilled water. The presence of the ssDNA may enhance the protonation of TMA.

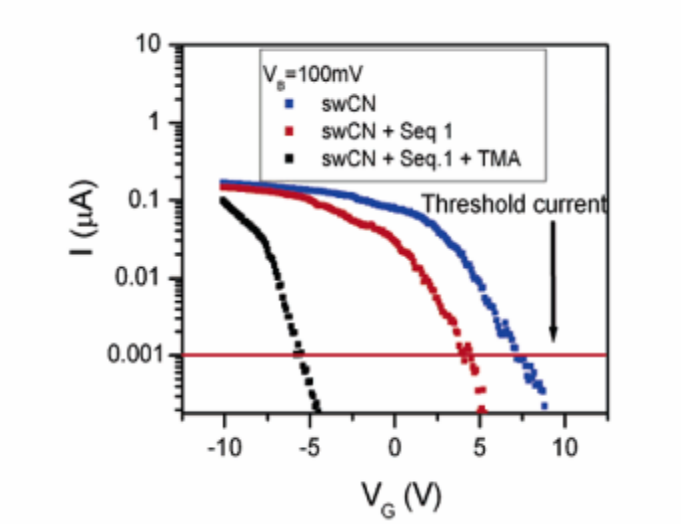

Figure 8.16: (a) Schematic of the carbon nanotube field-effect transistor functionalized with single-stranded DNA of two different sequences. The devices were exposed to the analytes in (b). (c) Transfer characteristics of the bare nanotube device, the device upon functionalization with ssDNA of sequence 1, and the functionalized device exposed to trimethylamine (TMA). *Figures from Ref. [Sta05].*

The enhanced response in the presence of ssDNA is not unique to TMA. Indeed, an enhanced response has been seen for several chemicals. In the case of methanol, the bare nanotube device shows essentially no response, but a strong decrease of the current is observed when the nanotube is functionalized with sequence 2; in addition, the response is reversible and repeatable. Similar experiments with TMA show that the presence of sequence 2 also enhances the response. The magnitude and sign of the current change is

specific to each analyte: a nanotube functionalized with sequence 1 shows a current reduction for methanol, and a current increase for propionic acid (Figure 8.17).

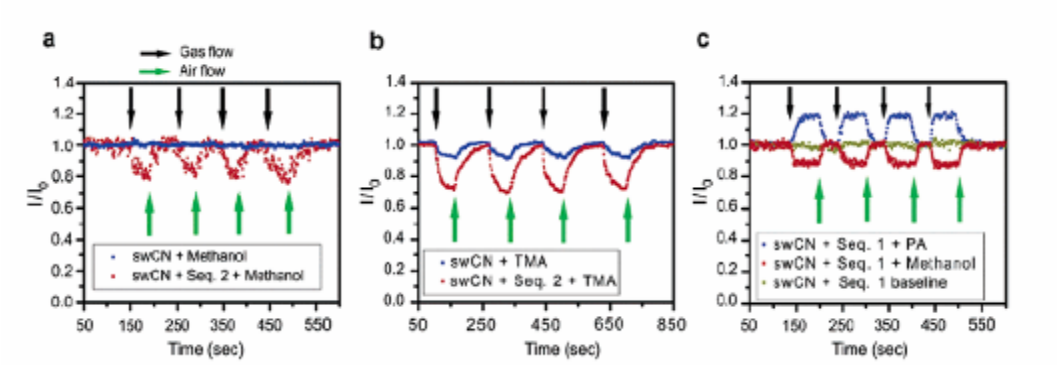

Figure 8.17: Current change of carbon nanotube field effect transistor when exposed to methanol, trimethyamine (TMA), and propionic acid (PA), with and without DNA functionalization of the nanotube. *Figure from Ref. [Sta05].*

The nanotube/ssDNA hybrids are also useful for the detection of chemicals used as simulants of explosives and nerve gas. (Detecting explosives is difficult because their low vaor pressure requires highly sensitive sensors.) Figure 8.18 shows the response of the nanotube device to dimethyl methylphosphonate (DMMP) and dinitrotoluene (DNT), simulants for explosives and nerve gases, respectively. As can be seen in the figure, the functionalized nanotubes show a strong response to each of these agents, while the bare nanotubes show no response. Moreover, the response is sequence-specific: at a concentration of 25 parts-per-million, DMMP gives a 7% reduction of the current with sequence 1, and a 14% reduction with sequence 2. Similar results are obtained with DNT.

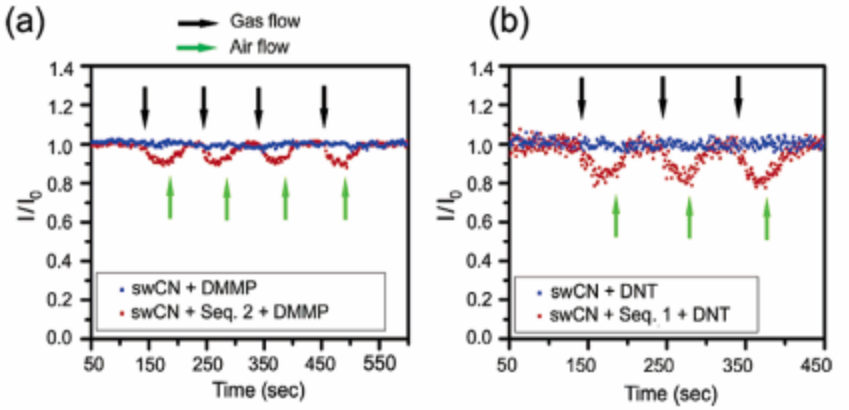

Figure 8.18: Change in current through a carbon nanotube field-effect transistor when exposed to dimethyl methylphosphonate (DMMP) and dinitrotoluene (DNT). The bare nanotube device shows no response to either agent, but functionalization with different ssDNA sequences gives a response for each gas. *Figure from Re. [Sta05].*

Other experiments with DNA-functionalized carbon nanotubes have focused on carbon nanotube network transistors [Sta06], with the aim of detecting single-nucleotide

mismatches in target DNA sequences. To demonstrate this ability, a combination of fluorescent imaging and electronic transport measurements were first performed to demonstrate the functionalization of the carbon nanotubes and the preferential attachment of a matched DNA sequence. Figure 8.19 shows a series of fluorescent microscopy images taken after functionalization with the capture DNA and after subsequent exposure to the target DNA. First, a DNA sequence of 5'-CCT AAT AAC AAT-3' labeled with a small fluorescent molecule was applied to the carbon nanotube network followed by a thorough washing to remove unbound DNA. The image in Figure 8.19A indicates that the DNA sequence attached predominantly to the carbon nanotubes (including over the electrodes), but not on the silicon dioxide substrate. The unlabelled capture sequence does not show any fluorescence (Figure 8.19B). Exposure of the carbon nanotube network functionalized with the unlabelled sequence to the fluorescent-labelled complimentary DNA sequence shows that the target DNA binds primarily to the carbon nanotube network (Figure 8.19C). When a different capture probe with little homology with the target probe is used, little fluorescence is observed from the carbon nanotube network (Figure 8.19E). These results indicate the ability to functionalizae the nanotube network, and the strong recognition capabilities of the ssDNA on the nanotube surface.

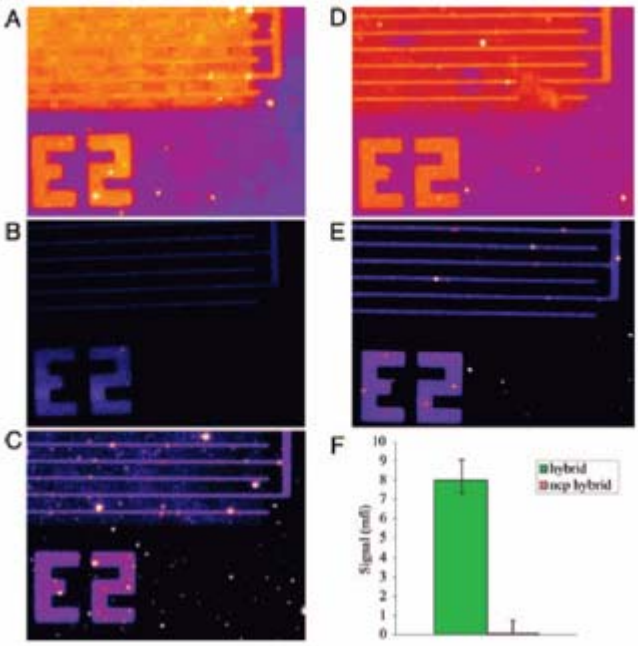

Figure 8.19: Fluorescence microscopy images of networks of carbon nanotubes between interdigitated electrodes after DNA incubation for one hour and removal of the unbound DNA oligomers. Image (A) was taken after incubation with 12-mer capture probes that were labeled with a fluorescent dye. Image (B) is for the same functionalization but without the dye. (C) Image taken after functionalization with the unlabelled capture sequence and exposure to the target sequence labeled with a fluorescent dye. (D) Image of the nanotube network functionalized with a different fluorescent-labelled DNA sequence. (E) A device functionalized with the non-labelled sequence of (D) has very low binding affinity to a mismatched fluorescent-labelled sequence. The graph in (F) shows the difference in the fluorescence intensity for capture of the complementary and non-complementary strands. *Figure from Ref. [Sta06].*

The binding of ssDNA to its complimentary strand can be observed by monitoring the changes in the transfer characteristics of the carbon nanotube network transistor. When functionalized with the capture probe, it is found that the ON state conductance is somewhat decreased from its value for the bare network, and that the threshold voltage is reduced by 2-5 V, consistent with the results presented earlier for the single nanotube devices. While exposure of the device to the non-complimentary ssDNA makes little difference in the transfer characteristics (Figure 8.20B), exposure to the complimentary strand gives a further shift of the threshold voltage by 1-2 V. These experiments demonstrate the ability to discriminate between two different DNA sequences using a rapid, label-free technique. Such approaches are currently being explored to enable the rapid diagnostic of diseases. As an example of the applicability of the carbon nanotube sensor for this purpose, it was utilized to detect single-nucleotide mutation in the HFE gene, which is responsible for hemochromatosis [Sta06]. In these experiments, the nanotubes were functionalized with 17-mer sequences of wild-type and mutant ssDNA which differ only in a single nucleotide. Hybridization with a 51-mer sequence containing the target sequence complimentary to the wild-type was conducted on devices with only the wild-type or the mutant capture probes. Measurement of the transfer characteristics (Figure 8.21) and fluorescence microscopy after washing show that little wild-type hybridization occurred on the mutant-functionalized nanotubes, while significant hybridization occurred on the wild-type-functionalized nanotubes, leading to a reduction of the ON state conductance and a reduction of the threshold voltage.

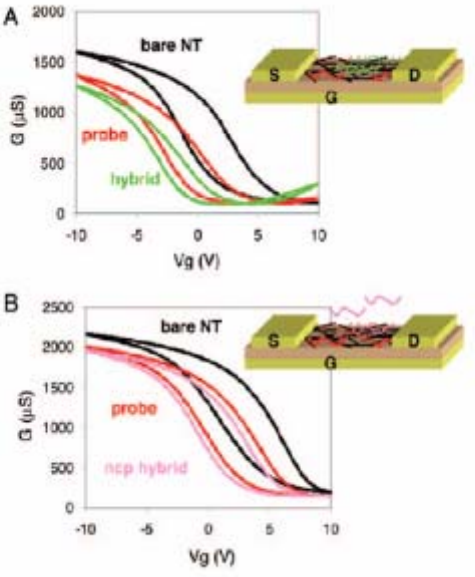

Figure 8.20: Transfer characteristics of a carbon nanotube network field-effect transistor when functionalized with ssDNA. Panel (A) shows the response to the complementary strand, while panel (B) is the response to a mismatched strand. *Figure from Ref. [Sta06].*

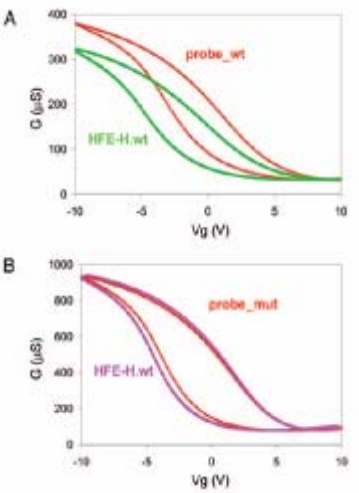

Figure 8.21: Response of ssDNA-functionalized carbon nanotube network transistor showing single-nucleotide discrimination between the wild-type (wt) and mutated (mut) forms of a target DNA sequence. *Figure from Ref. [Sta06].*

Many aspects of sensing with DNA-functionalized carbon nanotubes remain to be explored. The properties of the nanotube/ssDNA hybrid itself require further study to better understand the structure of the ssDNA, its impact on the nanotube electronic structure, the role of buffers, the importance of salts in the solution [Sta06], the differences between solution and on-chip functionalization, etc. Modeling work has been performed to address some of these issues [Lu05, Eny07]. Recent experiments [Tan06] have proposed that DNA hydridization at the contacts is the dominant sensing mechanism, with the changes in the transfer characteristics due to an increase of the Schottky barrier at the contact. In these experiments, Au was utilized as the contact material, and the increase in the Schottky barrier is believed to originate from a reduction of the Au workfunction upon hybridization on the Au surface. This conclusion is supported by quartz crystal microbalance and X-ray photoelectron spectroscopy on ssDNA-functionalized nanotubes dispersed on a substrate, which showed little binding of the complimentary strand.

8.2.2 Enzyme Coatings

In the first section of this chapter, we discussed liquid-gating of carbon nanotube transistors. By taking advantage of this approach, research has shown that enzyme-coated carbon nanotubes can serve as pH sensors, as well as to detect enzymatic activity [Bes03]. As shown in Figure 8.22, enzymes can be immobilized on carbon nanotubes through a linker molecule that binds non-covalently to the surface of carbon nanotubes. A particular example is the enzyme glucose oxidase which catalyses the oxidation of glucose. Attachment of this enzyme to the surface of carbon nanotubes results in a strong decrease of the conductance of the nanotube device (Figure 8.22B) when the conductance is measured in deionized water. Thus, this device is a good sensor for glucose oxidase in liquid. It was originally proposed that the sensing mechanism is the disruption of the

double-layer near the nanotube and the decrease of the capacitance of the liquid gate [Bes03]. However, rescaling of the gate voltage to represent this effect does not make the current-voltage curves overlap. Instead, a simple shift of the gate voltage gives excellent data overlap (inset in Figure 8.22B). Thus, it appears that charge transfer, as discussed in Section 8.1.1 is a likely mechanism to explain the experimental data.

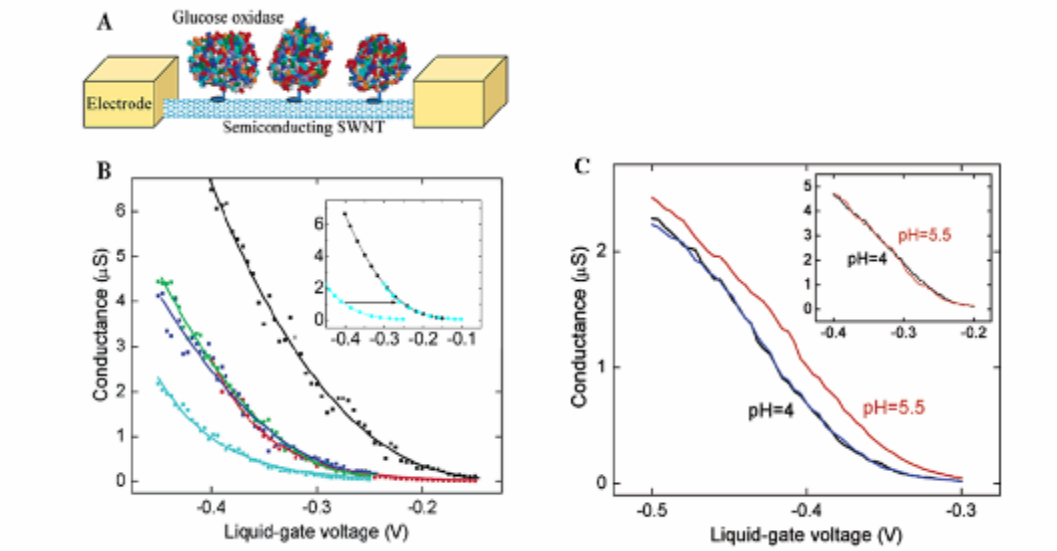

Figure 8.22: (A) Sketch of a carbon nanotube functinalized with the enzyme glucose oxidase. (B) The sequences of data from top to bottom correspond to the bare nanotube, the nanotube after soaking in DMF solution for 2 and 4 hours, after 2 hours in DMF with the linking molecule, and finally, after immobilization of glucose oxidase. The inset shows the collapse of the data for the bare nanotube and the enzyme-coated nanotube when the gate voltage is shifted. (C) Sensitivity of the enzyme-coated device to pH. Inset shows the response of the nanotube before immobilization of glucose oxidase. *Figures adapted from Ref. [Bes03].*

The enzyme-functionalized carbon nanotube field-effect transistors can be utilized to perform sensing in the liquid environment. For example, these devices are sensitive to the solution pH, with a decrease of the pH leading to a decrease of the conductance (Figure 8.22C). The impact of decreasing the pH on the transfer characteristics is a shift of the threshold voltage to more negative values, and it is proposed that charged groups on the glucose oxidase become less negatively charged in decreasing pH [Bes03]. It is also interesting to note that addition of glucose to the solution produced an increase of the device conductance, allowing the real-time detection of enzymatic activity.

8.2.3 Polymer Coatings

One strategy to impart specificity to carbon nanotube sensors is to cover the nanotube device with a polymeric layer that blocks most analytes except the targeted ones [Qi03, Star03b]. This strategy has been employed to achieve multiplex sensing of ammonia and nitrogen dioxide on a substrate containing multiple polymer-coated devices [Qi03]. An optical image of one of these devices is shown in Figure 8.23. There, three different carbon nanotube field-effect transistors have been microspotted with two different

polymers: polyethyleneimine (PEI) and Nafion (a polymeric perfluorinated sulfonic acid ionomer). Ammonia has a low affinity to PEI because of the high density of amines. Likewise, Nafion blocks species that do not contain –OH groups, such as nitrogen dioxide, but is permeable to molecules such as NH_3 which forms NO_4OH. These attributes were combined to selectively detect ammonia and nitrogen dioxide on separate devices. Figure 8.23 shows a time trace of the current flowing through two of the devices, one coated with PEI and the other coated with Nafion. Simultaneous exposure of both devices to NH_3 and NO_2 indicates that the PEI-coated device responds to NO_2 but not to NH_3; the reverse situation is observed for the Nafion-coated device.

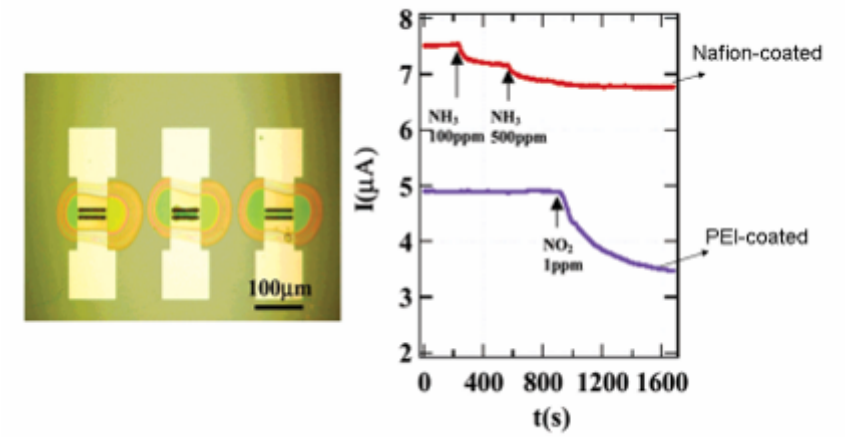

Figure 8.23: Multiplex detection of ammonia and nitrogen dioxide with carbon nanotubes coated with polymeric blocking layers. The optical image on the left shows three nanotube devices after each device is microspotted with droplets of different polymer solutions. The three devices are then simultaneously exposed to ammonia and nitrogen dioxide vapors. The right graph shows that the Nafion-coated nanotube device responds to ammonia but not to nitrogen dioxide, with the reverse response for the PEI-coated devices. *Figures from Ref. [Qi03].*

This strategy can be taken a step further by adding functionalization to the blocking layer [Sta03b, Che03]. In these cases, experiments to detect protein binding on carbon nanotubes indicated non-specific binding to the carbon nanotubes. To prevent this non-specific binding [Sta03b], a coating of polyethyleneglycol (PEG) and PEI was deposited on the nanotubes by submerging them in solution. The nanotube devices exhibited marked changes in their transfer characteristics after functionalization with these polymers. However, the initial *p*-type behavior can be recovered by adding a biotin functionalization to the polymeric layer. Biotin is a receptor molecule for the protein streptavidin, and the biotin-streptavidin system is often used as a model system for studies of protein binding. Functionalizing the polymeric layer with biotin allows streptavidin to bind covalently to the polymeric layer without disturbing the nanotube electronic properties. Demonstration of the viability of this approach is shown in Figure 8.24. In these figures, the transfer characteristincs of the carbon nanotube network transistor is shown for different functionalizations upon exposure to streptavidin. Panel b in this figure indicates that the bare nanotube device shows a response to streptavidin consisting of a reduction of the ON current and a shift of the threshold voltage. This type of behavior has been discussed above and is not specific to streptavidin. Coating the nanotube device with PEI/PEG completely blocks streptavidin (panel c) and the device

shows no response. However, when the PEI/PEG is functionalized with biotin, a large decrease of the current is observed, as indicated in Figure 8.24a. The actual mechanism that causes this strong sensing response is unclear. Increased scattering could certainly cause such an overall decrease of the current. However, the impact of the contacts has not been fully explored, and the modulation of Schottky barriers at the contacts could also play a role.

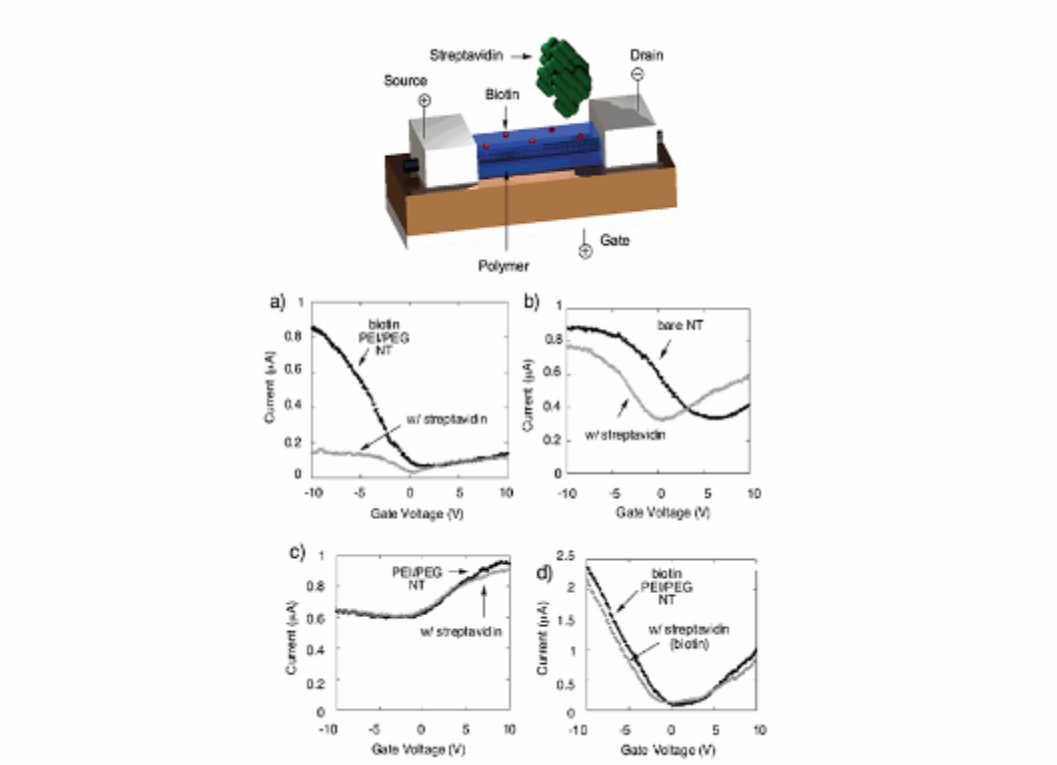

Figure 8.24: Schematic of a carbon nanotube field-effect transistor with a functionalized polymeric blocking layer. The bottom panels show the measured transfer characteristics of several nanotube devices with different functionalization before and after exposure to streptavidin. *Figures from Ref. [Sta03b].*

References

[Ade00] Ch. Adessi and M. Devel, "Theoretical study of field emission by single-wall carbon nanotubes", Phys. Rev. B **62**, R13314 (2000).

[Ago00] H. Ago, T. Kugler, F. Cacialli, W. R. Salaneck, M. S. P. Shaffer, A. H. Windle, R. H. Friend, "Work Functions and Surface Functional Groups of Multiwall Carbon Nanotubes", J. Phys. Chem. B **103,** 8116 (1999).

[Ana98] M. P. Anantram and T. R. Govindan, "Conductance of carbon nanotubes with disorder: a numerical study", Phys. Rev. B **58**, 4882 (1998).

[Ana00a] M. P. Anantram, "Current-carrying capacity of carbon nanotubes", Phys. Rev. B **62**, 4837 (2000).

[Ana00b] M. P. Anantram, S. Datta and Y. Xue, "Coupling of carbon nanotubes to metallic contacts", Phys. Rev. B **61**, 14219 (2000) .

[Ana01] M. P. Anantram, "Which nanowire couples better electrically to a metal contact: Armchair or zigzag nanotube?", Appl. Phys. Lett. **78**, 2055 (2001).

[Ana06] M. P. Anantram and F. Léonard, "Physics of carbon nanotube devices", Rep. Prog. Phys. **69**, 507 (2006).

[And98] T. Ando and T. Nakanishi, "Impurity scattering in carbon nanotubes – absence of back scattering", J. Phys. Soc. Jpn. **67**, 1704 (1998).

[And00] A. N. Andriotis, M. Menon, and G. E. Froudakis, "Various bonding configurations of transition-metal atoms on carbon nanotubes: Their effect on contact resistance", Appl. Phys. Lett. **76**, 3890 (2000).

[App02] J. Appenzeller, J. Knoch, V. Derycke, R. Martel, S. Wind and Ph. Avouris, "Field-modulated carrier transport in carbon nanotube transistors", Phys. Rev. Lett. **89**, 126801 (2002).

[App04] J. Appenzeller, M. Radosavljevic, J. Knoch, and Ph. Avouris, "Tunneling versus thermionic emission in one-dimensional semiconductors", Phys. Rev. Lett. **92**, 048301 (2004).

[Avr39] M. Avrami, "Kinetics of phase change. I General theory", J. Chem. Phys. **7**, 1103 (1939).

[Bac01] A. Bachtold, P. Hadley, T. Nakanishi, C. Dekker, "Logic circuits with carbon nanotube transistors", Science **294**, 1317 (2001).

[Bac02] S. M. Bachilo, M. S. Strano, C. Kittrell, R. H. Hauge, R. E. Smaley, R. B. Weisman, "Structure-assigned optical spectra of single-walled carbon nanotubes", Science **298**, 2361 (2002).

[Bes03] K. Besteman, J-O. Lee, F. G. M. Wiertz, H. A. Heering, and C. Dekker, "Enzyme-coated carbon nanotubes as single-molecule biosensors", Nano Lett. **3**, 727 (2003).

[Bau99] R. H. Baughman, C. Cui, A. A. Zakhidov, Z. Iqbal, J. N. Barisci, G. M. Spinks, G. G. Wallace, A. Mazzoldi, D. De Rossi, A. G. Rinzler, O. Jaschinski, S. Roth, M. Kertesz, "Carbon nanotube actuators", Science **284**, 1340 (1999).

[Bla75] J. M. Blakeley and J. C. Shelton, in "Surface Physics of Materials", edited by J. M. Blakeley (Academic, New York, 1975). Vol. 9, p. 208.

[Bla94] X. Blasé, L. X. Benedict, E. L. Shirley and S. G. Louie, "Hybridization effects and metallicity in small radius carbon nanotubes", Phys. Rev. Lett. **72**, 1878 (1994).

[Boc99a] M. Bockrath, D. H. Cobden, J. Lu, A. G. Rinzler, R. E. Smalley, L. Balents and P. L. McEuen, "Luttinger-liquid behaviour in carbon nanotubes", Nature **397**, 598 (1999).
[Boc99b] M. W. Bockrath, "Carbon nanotubes: Electrons in one dimension", Ph. D thesis, University of California, Berkeley, (1999).
[Bon99] J.-M. Bonard, J.-P. Salvetat, T. Stöckli, L. Forró, A. Châtelain, "Field emission from carbon nanotubes: perspectives for applications and clues to the emission mechanism", Applied Physics A: Materials Science & Processing **69**, 245 (1999).
[Bon01] J.-M. Bonard, T. Stöckli, O. Noury, and A. Châtelain, "Field emission from cylindrical carbon nanotube cathodes: Possibilities for luminescent tubes", Appl. Phys. Lett. **78**, 2775 (2001).
[Bon02] J.-M. Bonard, K. A. Dean, B. F. Coll, and C. Klinke, "Field emission of individual carbon nanotubes in the scanning electron microscope", Phys. Rev. Lett. **89**, 197602 (2002).
[Bon03] J.-M. Bonard, C. Klinke, K. A. Dean, B. F. Coll, "*Degradation and failure of carbon nanotube field emitters*", Phys. Rev. B **67**, 115406 (2003).
[Bos06] K. Bosnick, N. Gabor and P. McEuen, "Transport in carbon nanotube *p-i-n* diodes", Appl. Phys. Lett. **89**, 163121 (2006).
[Bou04] B. Bourlon, D. C. Glattli, B. Plaçais, J. M. Berroir, C. Miko, L. Forró, and A. Bachtold, "Geometrical dependence of high-bias current in multiwalled carbon nanotubes", Phys. Rev. Lett. **92**, 026804 (2004).
[Boy86] W. E. Boyce and R. C. DiPrima, "Elementary differential equations and boundary value problems", John Wiley and Sons (1986).
[Bul03] A. Buldum and J. P. Lu, "Electron field emission properties of closed carbon nanotubes". Phys. Rev. Lett. **91**, 236801 (2003).
[Bur02] P. J. Burke, "Luttinger liquid theory as a model of the GHz electrical properties of carbon nanotubes", IEEE Trans. Nanotechnol. **1**, 129 (2002).
[Cab03] I. Cabria, J. W. Mintmire and C. T. White, "Metallic and semiconducting narrow carbon nanotubes", Phys. Rev. B **67**, 121406 (2003).
[Cap05] R. B. Capaz, C. D. Spataru, P. Tangney, M. L. Cohen, S. G. Louie, "Temperature dependence of the band gap of semiconducting carbon nanotubes", Phys. Rev. Lett. **94**, 036801 (2005).
[Car97] D. L. Carroll, P. Redlich, P. M. Ajayan, J. C. Charlier, X. Blase, A. De Vita, and R. Car, "Electronic Structure and Localized States at Carbon Nanotube Tips", Phys. Rev. Lett. **78**, 2811 (1997).
[Cha04] E. Chang, G. Bussi, A. Ruini, and E. Molinari, "Excitons in carbon nanotubes: and ab initio symmetry-based approach", Phys. Rev. Lett. **92**, 196401 (2004).
[Che95] L. A. Chernozatonskii, Yu. V. Gulyaev, Z. Ja. Kosakovskaja, N. I. Sinitsyn, G. V. Torgashov, Yu. F. Zakharchenko, E. A. Fedorov and V. P. Val'chuk, "Electron field emission from nanofilament carbon films", Chem. Phys. Lett. **233**, 63 (1995).
[Che03] R. J. Chen, S. Bangsaruntip, K. A. Drouvalakis, N. Wong Shi Kam, M. Shim, Y. Li, W. Kim, P. J. Utz, and H. Dai, "Noncovalent functionalization of carbon nanotubes for highly specific electronic biosensors", Proc. Nat. Acad. Sci. **100**, 4984 (2003).
[Che04] R. J. Chen, H. C. Choi, S. Bangsaruntip, E. Yenilmez, X. Tang, Q. Wang, Y.-L. Chang, and H. Dai, "Investigation of the mechanisms of electronic sensing of protein adsorption on carbon nanotube devices", J. Am. Chem. Soc. **126**, 1563 (2004).

References

[Che05a] Z. Chen, J. Appenzeller, J. Knoch, Y.-M. Lin, and Ph. Avouris, "The role of metal-nanotube contact in the performance of carbon nanotube field-effect transistors", Nano Lett. **5**, 1497 (2005).

[Che05b] J. Chen, V. Perebeinos, M. Freitag, J. Tsang. Q. Fu, J. Liu, Ph. Avouris, "Bright infrared emission from electrically induced excitons in carbon nanotubes", Science **310**, 1171 (2005).

[Che06] Z. Chen, J. Appenzeller, Y.-M. lin, J. Sippel-Oakley, A. G. Rinzler, J. Tang, S. J. Wind, P. M. Solomon, P. Avouris, "An integrated logic circuit assembled on a single carbon nanotube", Science **311**, 1735 (2006).

[Chi02] L. F. Chibotaru, S. A. Bovin, and A. Ceulemans, "Bend-induced insulating gap in carbon nanotubes", Phys. Rev. B **66**, 161401(R) (2002).

[Cho99a] H. J. Choi, J. Ihm, Y-G Yoon, and S. G. Louie, "Possible explanation for the conductance of a single quantum unit in metallic carbon nanotubes", Phys. Rev. B **60**, R14009 (1999).

[Cho99b] W. B. Choi, D. S. Chung, J. H. Kang, H. Y. Kim, Y. W. Jin, I. T. Han, Y. H. Lee, J. E. Jung, N. S. Lee, G. S. Park, and J. M. Kim, "Fully sealed, high-brightness carbon-nanotube field-emission display", Appl. Phys. Lett. **75**, 3129 (1999).

[Cho07] W.-S. Cho, H.-J. Lee, Y.-D. Lee, J.-H. Park, J.-K. Kim, Y.-H. Lee, and B.-K. Ju, "Carbon nanotube-based triode field emission lamps using metal meshes with spacers", IEEE Elec. Dev. Lett. **28**, 386 (2007).

[Coh06] T. Cohen-Karni, L. Segev, O. Srur-Lavi, S. R. Cohen, and E. Joselevich, "Torsional electromechanical quantum oscillations in carbon nanotubes", Nat. Nano. **1**, 36 (2006).

[Col00] P. G. Collins, K. Bradley, M. Ishigami, A. Zettl, "Extreme oxygen sensivity of electronic properties of carbon nanotubes", Science **287**, 1801 (2000).

[Col01] P. G. Collins, M. Hersam, M. Arnold, R. Martel, and Ph. Avouris, "Current Saturation and Electrical Breakdown in Multiwalled Carbon Nanotubes"**,** Phys. Rev. Lett. **86**, 3128 (2001).

[Cro04] M. Croci, I. Arfaoui, T. Stöckli, A. Chatelain and J-M. Bonard, "A fully sealed luminescent tube based on carbon nanotube field emission", Microelectronics Journal **35**, 329 (2004).

[Cro06] S. B. Cronin, Y. Yin, A. Walsh, R. B. Capaz, A. Stolyarov, P. Tangney, M. L. Cohen, S. G. Louie, A. K. Swan, M. S. Ünlü, B. B. Goldberg, and M. Tinkham, "Temperature dependence of the optical transition energies of carbon nanotubes: the role of electron-phonon coupling and thermal expansion", Phys. Rev. Lett. **96**, 127403 (2006).

[Cui03] X. Cui, M. Freitag, R. Martel, L. Brus, and Ph. Avouris, "Controlling energy-level alignments at carbon nanotube/Au contacts", Nano Lett. **3**, 783 (2003).

[Cum00] J. Cummings and A. Zettl, "Low-friction nanoscale linear bearing realized from multiwall carbon nanotubes", Science **289**, 602 (2000).

[Cum02] J. Cummings, A. Zettl, M. R. McCartney, J. C. H. Spence, "Electron holography of field-emitting carbon nanotubes", Phys. Rev. Lett. **88**, 065804 (2002).

[Dea00] K. A. Dean and B. R. Chalamala, "Current saturation mechanisms in carbon nanotube field emitters", Appl. Phys. Lett. **76**, 375 (2000).

[Der01] V. Derycke, R. Martel, J. Appenzeller, Ph. Avouris, "Carbon nanotube inter- and intramolecular logic gates", Nano Lett. **292**, 453 (2001).

[Der02] V. Derycke, R. Martel, J. Appenzeller, Ph. Avouris, "Controlling doping and carrier injection in carbon nanotube transistors", Appl. Phys. Lett. **80**, 2773 (2002).
[Doy06] M. Doytcheva, M. Kaiser, and N. de Jonge, "*In-situ* transmission electron microscopy investigation of the structural changes in carbon nanotubes during electron emission at high currents", Nanotechnology **17**, 3226 (2006).
[Dre00] M. S. Dresselhaus and P. C. Eklund, "Phonons in carbon nanotubes", Adv. in Phys. **49**, 705 (2000).
[Dur04] T. Dürkop, S. A. Getty, E. Cobas, and M. S. Fuhrer, "Extraordinary mobility in semiconducting carbon nanotubes", Nano Lett. **4**, 35 (2004).
[Dut81] P. Dutta and P. M. Horn, "Low frequency fluctuations in solids: 1/*f* noise", Rev. Mod. Phys. **53**, 497 (1981).
[Eny07] A. N. Enyashin, S. Gremming, and G. Seifert, "DNA-wrapped carbon nanotubes", Nanotechnology **18**, 245702 (2007).
[Ese07] G. Esen, M. S. Fuhrer, M. Ishigami, E. D. Williams, "Transmission line impedance of carbon nanotube thin films for chemical sensing", Appl. Phys. Lett. **90**, 123510 (2007).
[Far04] A. A. Farijian, H. Mizuseki, Y. Kawazoe, "Electronic transport properties of a metal-semiconductor carbon nanotube heterojunction", Physica E **22**, 675 (2004).
[Fen03] A. M. Fennimore, T. D. Yusvinsky, W.-Q. Han, M. S. Fuhrer, J. Cumings, and A. Zettl, "Rotational actuators based on carbon nanotubes", Nature **424**, 408 (2003).
[Fow28] R. H. Fowler and L. W. Nordheim, "Electron emission in intense electric fields", Proc. Roy. Soc. Lond. **A119**, 173 (1928).
[Fra98] S. Frank P. Poncharal, Z. L. Wang, W. A. de Heer, "Carbon nanotube quantum resistors", Science **280**, 1744 (1998).
[Fre03] M. Freitag, Y. Martin, J. A. Misewich, R. Martel, Ph. Avouris,
"Photoconductivity of single carbon nanotubes", Nano Lett. **3**, 1067 (2003).
[Fre04] M. Freitag, J. Chen, J. Tersoff, J. C. Tsang, Q. Fu, J. Liu, and Ph. Avouris,
"Mobile ambipolar domain in carbon-nanotube infrared emitters", Phys. Rev. Lett. **93**, 076803 (2004).
[Fre05] M. Freitag, J. Tersoff, J. Chen, J. C. Tsang, Ph. Avouris, "Electroluminescence in carbon nanotubes", AIP Conf. Proc. **786**, 477 (2005).
[Fuh00] M. S. Fuhrer, J. Nygård, L. Shih, M. Forero, Y-G. Yoon, M. S. C. Mazzoni, H. J. Choi, J. Ihm, S. G. Louie, A. Zettl, and P. L. McEuen, "Crossed nanotube junctions", Science **288**, 494 (2000).
[Gar03] Yu. N. Gartstein, A. A. Zakhidov, and R. H. Baughman, "Mechanical and electromechanical coupling in carbon nanotube distortions", Phys. Rev. B **68**, 115415 (2003).
[Gom04] C. Gómez-Navarro, P.J. de Pablo, J. Gómez-Herrero, "Radial electromechanical properties of carbon nanotubes", Adv. Mat. **16**, 549 (2004).
[Gra01] E. Graugnard, P. J. dePablo, B. Walsh, A. W. Ghosh, S. Datta, R. Reifenberger, "Temperature dependence of the conductance of multiwalled carbon nanotubes", Phys. Rev. B **64**, 125407 (2001).
[Gru03] M. Grujicic, G. Cao, R. Singh, "The effect of topological defects and oxygen adsorption on the electronic transport properties of single-walled carbon-nanotubes", Appl. Surf. Sci. **211**, 166 (2003).

[Gul02] O. Gülseren, T. Yildirim, S. Ciraci, and Ç. Kılıç, "Reversible band-gap engineering in carbon nanotubes by radial deformation", Phys. Rev. B **65**, 155410 (2002).
[Gul05] D. Guldi, H. Taieb, G. M. A. Rahman, N. Tagmatarchis, M. Prato, "Novel photoactive single-wall carbon nanotube-porphyrin polymer wraps: Efficient and long-lived intracomples charge separation", Adv. Mater. **17**, 871 (2005).
[Guo05] X. Guo, L. Huang, S. O'Brien, P. Kim, and C. Nuckolls, "Directing and sensing changes in molecular conformation on individual carbon nanotube field effect transistors", J. Am. Chem. Soc. **127**, 15045 (2005).
[Ham37] L. P. Hammett, "The Effect of Structure upon the reactions of organic compounds. Benzene derivatives" J. Am. Chem. Soc. **59**, 96 (1937).
[Har90] W. A. Harrison, "Electronic structure and the properties of solids: The physics of the chemical bond", Freeman, San Francisco (1990).
[Hec06] D. S. Hecht, R. A. Ramirez, E. Artukovic, M. Briman, K. Chichak, J. F. Stoddart, G. Grüner, "Bioinspired detection of light using a porphyrin-sensitized single-wall nanotube field effect transistor", Nano Lett. **6**, 2031 (2006).
[Hee95] W. A. de Heer, A. Chatelain and D. Ugarte, "A carbon nanotube field-emission electron source", Science **270**, 1179 (1995).
[Hei02] S. Heinze, J. Tersoff, R. Martel, V. Derycke, J. Appenzeller, Ph. Avouris, "Carbon nanotubes as Schottky barrier transistors", Phys. Rev. Lett. **89**, 106801 (2002).
[Hei03] S. Heinze, M. Radosavljevic, J. Tersoff, and Ph. Avouris, "Unexpected scaling of the performance of carbon nanotube transistors", Phys. Rev. B **68**, 235418 (2003).
[Hey97] R. Heyd, A. Charlier, and E. McRae, "Uniaxial-stress effects on the electronic properties of carbon nanotubes", Phys. Rev. B **55**, 6820 (1997).
[Hoo69] F. N. Hooge, "1/f noise is no surface effect", Phys. Lett. A **29**, 139 (1969).
[Hua04] N. Y. Hua, J. C. She, J. Chen, S. Z. Deng, N. S. Xu, H. Bishop, S. E. Huq, L. Wang, D. Y. Zhong, E. G. Wang, and D. M. Chem, "Mechanism responsible for initiating carbon nanotube vacuum breakdown", Phys. Rev. Lett. **93**, 075501 (2004).
[Ish06] M. Ishigami, J. H. Chen, E. D. Williams, D. Tobias, Y. F. Chen, and M. S. Fuhrer, "Hooge's constant for carbon nanotube field effect transistors", Appl. Phys. Lett. **88**, 203116 (2006).
[Itk06] M. E. Itkis, F. Borondics, A. Yu, R. C. Haddon, "Bolometric infrared photoresponse of suspended single-walled carbon nanotube films", Science **312**, 413 (2006).
[Jav02a] A. Javey, H. Kim, M. Brink, Q. Wang, A. Ural, J. Guo, P. Mcintyre, P. Mceuen, M. Lundstrom, and H. Dai, "High-κ dielectrics for advanced carbon nanotube transistors and logic gates", Nat. Mater. **1**, 241 (2002).
[Jav02b] A. Javey, Q. Wang, A. Ural, Y. Li, and H. Dai, "Carbon nanotube transistor arrays for multistage complimentary logic and ring oscillators", Nano Lett. **2**, 929 (2002).
[Jav03] A. Javey, J. Guo, Q. Wang, M. Lundstrom and H. Dai, "Ballistic carbon nanotube field-effect transistors", Nature **424**, 654 (2003).
[Jen06] K. Jensen, C. Girit, W. Mickelson, and A. Zettl, "Tunable nanoresonators constructed from telescoping nanotubes", Phys. Rev. Lett. **96**, 215503 (2006).
[Jis93] R. A. Ishi, L. Venkataraman, M. S. Dresselhaus, and G. Dresselhaus, "Phonon modes in carbon nanotubules", Chem Phys. Lett. **209**, 77 (1993).

[Joh03] D. L. John, C. Castro, and D. L. Pulfrey, "Electrostatics of coaxial Schottky-barrier field-effect transistors", IEEE Trans. Nano. **2** 175 (2003).
[Jon02] N. de Jonge, Y. Lamy, K. Schoots, and T. H. Oosterkamp, "High brightness electron beam from a multi-wall carbon nanotube", Nature **420**, 393 (2002).
[Jon04a] N. de Jonge, M. Allioux, M. Doytcheva, M. Kaiser, K.B.K. Teo, R.G. Lacerda and W.I. Milne, "Characterization of the field emission properties of individual thin carbon nanotubes", Appl. Phys. Lett. **85**, 1607 (2004).
[Jon04b] N. de Jonge and J.-M. Bonard, "Carbon nanotube electron sources and applications", Phil. Trans. R. Soc. Lond. A **362**, 2239 (2004).
[Kil00] Ç. Kılıç, S. Ciraci, O. Gülseren, and T. Yildirim, "Variable and reversible quantum structures on a single carbon nanotube"**,** Phys. Rev. B **62**, 16345 (2000).
[Kim05] W. Kim, A. Javey, R. Tu. J. Cao, Q. Wang, and H. Dai, "Electrical contacts to carbon nanotubes down to 1 nm in diameter", Appl. Phys. Lett. **87**, 173101 (2005).
[Kle01] A. Kleiner and S. Eggert, "Band gaps of primary metallic carbon nanotubes"**,** Phys. Rev. B **63**, 73408 (2001).
[Kon00] J. Kong, N. R. Franklin, C. Zhou, M. G. Chapline, S. Peng, K. Cho, and H. Dai, "Nanotube molecular wires as chemical sensors", Science **287**, 622 (2000).
[Kon01a] J. Kong, E. Yenilmez, T. W. Tombler, W. Kim, H. Dai, R. B. Laughlin, L. Liu, C. S. Jayanthi, and S. Y. Wu, "Quantum interference and ballistic transmission in nanotube electron waveguides", Phys. Rev. Lett. **87**, 106801, (2001).
[Kon01b] J. Kong, M. G. Chapline, and H. Dai, "Functionalized carbon nanotubes for moleculer hydrogen sensors", Adv. Mater. **13**, 1384 (2001).
[Kre02] F. Kreupl, A. P. Graham, G. S. Duesberg, W. Steinhogl, M. Liebau, E. Unger, and W. Honlein, "Carbon nanotubes in interconnect applications", Microelectron. Eng. **64**, 399 (2002).
[Kwo04] Y.-K. Kwon, S. Berber, and D. Tomanek, "Thermal contraction of carbon fullerenes and nanotubes", Phys. Rev. Lett. **92**, 015901 (2004).
[Lan57] R. Landauer, "Spatial variation of currents and fields due to localized scatterers in metallic conduction", IBM J. Res. Dev. **1** (3), 223 (1957).
[Lar06] L. Larrimore, S. Nad, X. Zhou, H. Abruna, and P. M. McEuen, "Probing electrostatic potentials in solution with carbon nanotube transistors", Nano Lett. **6**, 1329 (2006).
[Lat05] S. Latil, S. Roche, and J.-C. Charlier, "Electronic transport in carbon nanotubes with random coverage of physisorbed molecules", Nano Lett. **5**, 2216 (2005).
[Lee04] J. U. Lee, P. P. Gipp and C. M. Heller, "Carbon nanotube *p-n* junction diodes", Appl. Phys. Lett. **85,** 145 (2004).
[Lee05] J. U. Lee, "Photovoltaic effect in ideal carbon nanotube diodes", Appl. Phys. Lett. **87**, 073101 (2005).
[Lee07a] J. U. Lee, "Band-gap renormalization in carbon nanotubes: Origin of the ideal diode behavior in carbon nanotube *p-n* structures", Appl. Phys. Lett. **87**, 073101 (2005).
[Lee07b] J. U. Lee, P. J. Codella, and M. Pietrzykowski, "Direct probe of excitonic and continuum transitions in the photocurrent spectroscopy of individual carbon nanotube *p-n* diodes", Appl. Phys. Lett. **90**, 053103 (2007).
[Lef04] J. Lefebvre, P. Finnie, and Y. Homma, "Temperature-dependent photoluminescence from single-walled carbon nanotubes", Phys. Rev. B **70**, 045419 (2004).

[Leo99] F. Léonard and J. Tersoff, "Novel length scales in nanotube devices", Phys. Rev. Lett. **83**, 5174 (1999).
[Leo00a] F. Léonard and J. Tersoff, "Role of Fermi-level pinning in nanotube Schottky diodes", Phys. Rev. Lett. **84** 4693 (2000).
[Leo00] F. Léonard and J. Tersoff, "Negative differential resistance in nanotube devices", Phys. Rev. Lett. **85**, 4767 (2000).
[Leo02a] F. Léonard and J. Tersoff, "Multiple functionality in nanotube transistors", Phys. Rev. Lett. **88**, 258302 (2002).
[Leo02b] F. Léonard and J. Tersoff, "Dielectric response of semiconducting carbon nanotubes", Appl. Phys. Lett. **81**, 4835 (2002).
[Leo03] F. Léonard, "Quantum transport in nanotube transistors", Phys. Stat. Sol. (b) **239**, 88 (2003).
[Leo05] F. Léonard, F. E. Jones, A. A. Talin, and P. M. Dentinger, "Robustness of nanotube electronic transport to conformational deformations", Appl. Phys. Lett., **86**, 093112 (2005).
[Leo06a] F. Léonard, "Size-Dependent Effects on Electrical Contacts to Nanotubes and Nanowires", Phys. Rev. Lett. **97**, 026804 (2006).
[Leo06b] F. Léonard and D. A. Stewart, "Properties of short channel ballistic carbon nanotube transistors with ohmic contacts", Nanotechnology **17**, 4699 (2006).
[Leo06c] F. Léonard, "Crosstalk between nanotube devices: contact and channel effects", Nanotechnology **17**, 2381 (2006).
[Lia04] Y. X. Liang, Q. H. Li, and T. H. Wang, "Current saturation in multiwalled carbon nanotubes by large bias", Appl. Phys. Lett. **84**, 3379 (2004).
[Lin01] S. Y. Lin, R. Y. Tsai, S. C. Lee, "High-performance InAs/GaAs quantum-dot infrared photodetectors with a single-sided $Al_{0.3}Ga_{0.7}As$ blocking layer", Appl. Phys. Lett. 78, 2784 (2001).
[Liu00] L. Liu, C. S. Jayanthi, M. Tang, S. Y. Wu, T. W. Tombler, C. Zhou, L. Alexseyev, J. Kong, and H. Dai, "Controllable reversibility of an sp2 to sp3 transition of a single wall nanotube under the manipulation of an AFM Tip: A nanoscale electromechanical switch?", Phys. Rev. Lett. **84**, 4950 (2000).
[Liu03] Y. Liu, "Ab initio study of Ti-contacted single-walled carbon nanotube"**,** Phys. Rev. B **68**, 193409 (2003).
[Lou03] R. Loucif-Saibi, K. Nakatani, and J. A. Delaire, M. Dumont and Z. Sekkat, "Photoisomerization and second harmonic generation in disperse red one-doped and –functionalized poly(methy1 methacrylate) films", Chem. Mater. **5**, 229 (1993).
[Lov00] D. Lovall, M. Buss, E. Graugnard, R. P. Andres, and R. Reifenberger, "Electron emission and structural characterization of a rope of single-walled carbon nanotubes", Phys. Rev. B **61**, 5683 (2000).
[Lov04] M. N. Lovellette, A. B. Campbell, H. L. Hughes, R. K. Lawrence, J. W. Ward, M. Meinhold, T. R. Bengston, G. F. Carleton, B. M. Segal, T. Rueckes, "Nanotube memories for space applications", Proc. 2004 IEEE Aero. Conf., p. 2300 (2004).
[Lu03] J.-Q. Lu, J. Wu, W. Duan, F. Liu, B.-F. Zhu, and B.-L. Gu, "Metal-to-semiconductor transition in squashed armchair carbon nanotubes", Phys. Rev. Lett. **90**, 156601 (2003).
[Lu05] G. Lu, P. Maragakis, and E. Kaxiras, "Carbon nanotube interaction with DNA", Nano Lett. **5**, 897 (2005).

[Lu06] Y. Lu, S. Bangsaruntip, X. Wang, L. Zhang, Y. Nishi, H. Dai, "DNA functionalization of carbon nanotubes for ultrathin atomic layer deposition of high κ dielectrics for nanotube transistors with 60 mV/decade switching", J. Am. Chem. Soc. **128**, 3158 (2006).
[Mai02] A. Maiti, A. Svizhenko and M. P. Anantram, "Electronic transport through carbon nanotubes: Effects of structural deformation and tube chirality", Phys. Rev. Lett. **88**, 126805 (2002).
[Man07] D. Mann, Y. K. Kato, A. Kinkhabwala, E. Pop, J. Cao, X. Wang, L. Zhang, Q. Wang, J. Guo, and H. Dai, "Electrically driven thermal light emission from individual single-walled carbon nanotubes", Nature Nanotech. **2**, 33 (2007).
[Mar98] R. Martel, T. Schmidt, H. R. Shea, T. Hertel, and Ph. Avouris, "Single- and multi-wall carbon nanotube field-effect transistors", Appl. Phys. Lett. **73**, 2447 (1998).
[Mar01] R. Martel, V. Derycke, C. Lavoie, J. Appenzeller, K. K. Chan, J. Tersoff, and Ph. Avouris, "Ambipolar electrical transport in semiconducting single-wall carbon nanotubes", Phys. Rev. Lett. **87**, 256805 (2001).
[Mar06a] M. S. Marcus, J. M. Simmons, O. M. Castellini, R. J. Hamers, and M. A. Eriksson "Photo-gating carbon nanotube transistors", J. Appl. Phys. **100**, 084306 (2006).
[Mar06b] L. Marty, E. Adams, L. Albert, R. Doyon, D. Ménard, and R. Martel, "Exciton formation and annihilation during 1D impact excitation of carbon nanotubes", Phys. Rev. Lett. **96**, 136803 (2006).
[McW57] A. L. McWhorter, in "Semiconductor surface physics", Ed. R. H. Kingston, University of Pennsylvania Press, Philadephia 1957.
[Meh05] H. Mehrez, A. Svizhenko, M. P. Anantram, M. Elstner, and T. Frauenheim, "Analysis of band-gap formation in squashed armchair carbon nanotubes", Phys. Rev. B **71**, 155421 (2005).
[Min98] J.W. Mintmire and C. T. White, "Universal density of states for carbon nanotubes", Phys. Rev. Lett. **81**, 2506 (1998).
[Min03] E. D. Minot, Y. Yaish, V. Sazonova, J-Y. Park, M. Brink, and P. L. McEuen, "Tuning Carbon Nanotube Band Gaps with Strain", Phys. Rev. Lett. **90**, 156401 (2003).
[Mis03] J. A. Misewich, R. Martel, Ph. Avouris, J. C. Tsang, S. Heinze, J. Tersoff, "Electrically induced optical emission from a carbon nanotube FET", Science **300**, 783 (2003).
[Nar99] M. B. Nardelli and J. Bernnholc, "Mechanical deformations and coherent transport in carbon nanotubes", Phys. Rev. B **60**, R16338 (1999).
[Nem06] N. Nemec, D. Tománek, and G. Cuniberti, "Contact dependence of carrier injection in carbon nanotubes: An ab initio study", Phys. Rev. Lett. **96**, 076802 (2006).
[Ngo04] Q. Ngo, D. Petranovic, S. Krishnan, A. M. Cassell, Q. Ye, J. Li, M. Meyyappan, and C. Y. Yang, "Electron transport through metal-multiwall carbon nanotube interfaces", IEEE Trans. Nanotechnol. **3**, 311 (2004).
[Nil00] L. Nilsson, O. Groening, C. Emmenegger, O. Kuettel, E. Schaller, L. Schlapbach, H. Kind, J-M. Bonard, and K. Kern, "Scanning field emission from patterned carbon nanotube films", Appl. Phys. Lett. **76**, 2071 (2000).
[Nos06] Y. Nosho, Y. Ohno, S. Kishimoto, and T. Mizutani, "Relation between conduction property and work function of contact metal in carbon nanotube field-effect transistor", Nanotechnology **17**, 3412 (2006).

[Odi00] A. Odintsov, “Schottky barriers in carbon nanotube heterojunctions”, Phys. Rev. Lett. **85**, 150 (2000).
[Oh00] S.-H. Oh, D. Monroe, and J. M. Hergenrother, IEEE Electron Device Lett. **21** 445 (2000).
[Pal03] J. J. Palacios, A. J. Pérez-Jiménez, E. Louis, E. SanFabián, and J. A. Vergés, “First-principles phase-coherent transport in metallic nanotubes with realistic contacts”, Phys. Rev. Lett. **90**, 106801 (2003).
[Par99] C. J. Park, Y. H. Kim, and K. J. Chang, “Band-gap modification by radial deformation in carbon nanotubes”, Phys. Rev. B **60**, 10656 (1999).
[Par04] J. Park, S. Rosenblatt, Y. Yaish, V. Sazonova, H. Ustunel, S. Braig, T. A. Arias, P. W. Brouwer, and P. L. McEuen, “Electron-phonon scattering in metallic single-walled carbon nanotubes”, Nano Lett. **4**, 517 (2004).
[Par05] N. Park and S. Hong, “Electronic structure calculations of metal-nanotube contacts with or without oxygen adsorption”, Phys. Rev. B **72**, 045408 (2005).
[Pau99] S. Paulson, M. R. Falvo, N. Snider, A. Helser, T. Hudson, A. Seeger, R. M. Taylor, R. Superfine, and S. Washburn, “*In situ* resistance measurements of strained carbon nanotubes”, Appl. Phys. Lett. **75**, 2936 (1999).
[Pen06] H. B. Peng, C. W. Chang, S. Aloni, T. D. Yuzvinsky, and A. Zettl, “Ultrahigh frequency nanotube resonators”, Phys. Rev. Lett. **97**, 087203 (2006).
[Per04] V. Perebeinos, J. Tersoff, Ph. Avouris, “Scaling of excitons in carbon nanotubes”, Phys. Rev. Lett. **92**, 257402 (2004).
[Per05] V. Perebeinos, J. Tersoff, Ph. Avouris, “Electron-phonon interaction and transport in semiconducting carbon nanotubes”, Phys. Rev. Lett. **94**, 086802 (2005).
[Per06] V. Perebeinos, J. Tersoff, Ph. Avouris, “Mobility in semiconducting carbon nanotubes at finite carrier density”, Nano Lett. **6**, 205 (2006).
[Per07] V. Perebeinos, Ph. Avouris, “Exciton ionization, Franz-Keldysh and Stark effects in carbon nanotubes’, Nano Lett. **7**, 609 (2007).
[Phi06] “Basic research needs for solid state lighting”, Report of the Basic Energy Sciences Workshop on Solid State Lighting, Office of Science, United States Department of Energy (2006).
[Pon02] P. Poncharal, C. Berger, Y. Yi, Z. L. Wang, and W. A. de Heer, J. Phys. Chem. B **106**, 12104 (2002).
[Pop05] E. Pop, D. Mann, J. Cao, Q. Wang, K. Goodsen, and H. Dai, “Negative differential conductance and hot phonons in suspended nanotube molecular wires”, Phys. Rev. Lett. **95**, 155505 (2005).
[Pur02] S. T. Purcell, P. Vincent, C. Journet and V. T. Binh, “Hot nanotubes: Stable heating of individual multiwall carbon nanotubes to 2000 K induced by the field-emission current”, Phys. Rev. Lett. **88**, 105502 (2002).
[Qi03] P. Qi, O. Vermesh, M. Grecu, A. Javey, Q. Wang, and H. Dai, “Towad large arrays of multiplex functionalized carbon nanotube sensors for highly selective and selective molecular detection”, Nano Lett. **3**, 347 (2003).
[Rar02] N. R. Raravikar, P. Keblinski, A. M. Rao, M. S. Dresselhaus, L.
S. Schadler, and P. M. Ajayan, “Temperature dependence of radial breathing mode Raman frequency of single-walled carbon nanotubes”, Phys. Rev. B **66**, 235424 (2002).

[Rin95] A. G. Rinzler, J. H. Hafner, P. Nikolaev, L. Lou, S. G. Kim, D. Tomanek, P. Nordlander, D. T. Colbert and R. E. Smalley, “Unraveling nanotubes: Field emission from an atomic wire," Science **269**, 1550 (1995).
[Roc99] A. Rochefort , P. Avouris, F. Lesage, and D. Salahub, “Electrical and mechanical properties of distorted carbon nanotubes”, Phys. Rev. B **60**, 13824 (1999).
[Rue00] T. Rueckes, K. Kim, E. Joselevich, G. Y. Tseng, C-L Cheung, and C. M. Lieber, “Carbon nanotube-based nonvolatile random access memory for molecular computing”, Science **289**, 94 (2000).
[Rui02] A. Ruini, M. J. Caldas, G. Bussi, and E. Molinari, “Solid state effects on exciton states and optical properties of PPV”, Phys. Rev. Lett. **88**, 206403 (2002).
[Sai00] R. Saito, G. Dresselhaus, M. S. Dresselhaus, “Trigonal warping effect of carbon nanotubes”, Phys. Rev. B **61**, 2981 (2000).
[Sai05] R. Saito, G. Dresselhaus, M. S. Dresselhaus, “Physical properties of carbon nanotubes”, Imperial College Press, London, UK (2005).
[San00] S. Sanvito, Y. K. Kwon, D. Tomanek, and C. J. Lambert, “Fractional Quantum Conductance in Carbon Nanotubes”, Phys. Rev. Lett. **84**, 1974 (2000).
[Sap03] S. Sapmaz, Ya. M. Blanter, L. Gurevich, and H. S. J. van der Zant, “Carbon nanotubes as nanoelectromechanical systems”, Phys. Rev. B **67**, 235414 (2003).
[Sar04] P. Sarrazin, D. Blake, L. Delzeit, M. Meyyappan, B. Boyer, S. Snyder, and B. Espinosa, “Carbon-nanotube field emission X-ray tube for space exploration XRD/XRF instrument”, *Adv. X-Ray Anal.***46**, 232 (2004).
[Sar05] P. Sarrazin, D. Blake, S. Feldman, S. Chipera, D. Vaniman, and D. Bish, “Field deployment of a portable X-ray diffraction/X-ray fluorescence instrument on Mars analog terrain”, *Adv. X-Ray Anal.* **48**, 194 (2005).
[Saz04] V. Sazonova, Y. Yaish, H. Ustunel, D. Roundy, T. A. Arias, P. L. McEuen, “A tunable carbon nanotube electromechanical oscillator”, Nature **431**, 284 (2004).
[Sim07] J. Simmons, I. In, V. E. Campbell, T. J. Mark, F. Léonard, P. Gopalan, and M. A. Eriksson, “Optically modulated conduction in chromophore-functionalized single wall carbon nanotubes”, Phys. Rev. Lett. **98**, 086802 (2007).
[Sno05] E. S. Snow, F. K. Perkins, E. J. Houser, S. C. Badescu, T. L. Reinecke, “Chemical detection with a single-walled carbon nanotube capacitor”, Science **307**, 1942 (2005).
[Spa04] C. D. Spataru, S. Ismail-Beigi, L. X. Benedict, and S. G. Louie, “Excitonic effects and optical spectra of single-walled carbon nanotubes”, Phys. Rev. Lett. **92**, 077402 (2004).
[Spa05] C. D. Spataru, S. Ismail-Beigi, L. X. Benedict, and S. G. Louie, “Excitonic effects and optical spectra of single-walled carbon nanotubes”, AIP Conf. Proc. **772**, 1061 (2005).
[Sta03a] A. Star, T.-R. Han, J.-C. P. Gabriel, K. Bradley, and G. Grüner, “Interaction of aromatic compounds with carbon nanotubes: correlations to the Hammett parameter of the substituent and measured carbon nanotube FET response”, Nano Lett. **3**, 1421 (2003).
[Sta03b] A. Star, J.-C. P. Gabriel, K.l Bradley, and G. Grüner, “Electronic detection of specific protein binding using nanotube FET devices”, Nano Lett. **3**, 459 (2003).
[Sta05] C. Staii, A. T. Johnson, M. Chen, A. Gelperin, “DNA-decorated carbon nanotubes for chemical sensing”, Nano Lett. **5**, 1774 (2005).

[Sta06] A. Star, E. Tu, J. Niemann, J.-C. P. Gabriel, C. S. Joiner, and C. Valcke, "Label-free detection of DNA hybridization using carbon nanotube network field-effect transistors", P. Nat. Acad. Sci. **103**, 921 (2006).
[Ste04] D. A. Stewart and F. Léonard, "Photocurrents in nanotube junctions", Phys. Rev. Lett. **93**, 107401 (2004).
[Ste05] D. A. Stewart and F. Léonard, "Energy conversion efficiency in nanotube optoelectronics", Nano Lett. **5**, 219 (2005).
[Sti05] G. Stix, "Nanotubes in the clean room", Scientific American, p. 82, February (2005).
[Sug01] H. Sugie, M. Tanemura, V. Filip, K. Iwata, K. Takahashi, and F. Okuyama, "Carbon nanotubes as electron source in an x-ray tube", Appl. Phys. Lett. **78**, 2578 (2001).
[Suz00] S. Suzuki, C. Bower, and Y. Watanabe, "Work functions and valence band states of pristine and Cs-intercalated single-walled carbon nanotube bundles", Appl. Phys. Lett. **76,** 4007 (2000).
[Svi05] A. Svizhenko and M. P. Anantram, "Effect of scattering and contacts on current and electrostatics in carbon nanotubes", Phys. Rev. B **72**, 085430 (2005).
[Sze81] S. M. Sze, "Physics of Semiconductor Devices", John Wiley & Sons (1981).
[Tal01] A. A. Talin *et al*, "", Solid. State Elec. **45**, 963 (2001).
[Tal04] A. A. Talin, P. M. Dentinger, F. E. Jones, S. Pathak, L. Hunter, F. Léonard, and A. M. Morales, "Assembly and electrical characterization of DNA-wrapped carbon nanotube devices", J. Vac. Sci. Technol. B **22**, 3107 (2004).
[Tal06a] F. E. Jones, A. A. Talin, F. Léonard, P. M. Dentinger, M. W. Clift, "Effect of electrode material on transport and chemical sensing characteristics of metal/carbon nanotube contacts", J. Electron. Mater. **35**, 1641 (2006).
[Tal06b] A. A. Talin, L. L. Hunter, F. Léonard, and B. Rokad, "Large area, dense silicon nanowire array chemical sensors", Appl. Phys. Lett. **89**, 153102 (2006).
[Tan98] S. J. Tans, A. R. M. Verschueren and C. Dekker, "Room-temperature transistor based on a single carbon nanotube", Nature **393**, 49 (1998).
[Tan06] X. Tang, S. Bansaruntip, N. Nakayama, E. Yenilmez, Y.-I. Chang, and Q. Wang, "Carbon nanotube DNA sensor and sensing mechanism", Nano Lett. **6**, 1632 (2006).
[Tar01] R. Tarkiainen, M. Ahlskog, J. Penttilä, L. Roschier, P. Hakonen, M. Paalanen, and E. Sonin, "Multiwalled carbon nanotube: Luttinger versus Fermi liquid", Phys. Rev. B **64**, 195412 (2001).
[Tch06] A. Tchernatinsky, S. Desai, G. U. Sumanasekera, C. S. Jayanthi, S. Y. Wu, B. Nagabhirava, and B. Alphenaar, "Adsorption of oxygen molecules on individual single-wall carbon nanotubes", J. Appl. Phys. **99**, 034306 (2006).
[Ter94] J. Tersoff and R. S. Ruoff, "Structural properties of a carbon-nanotube crystal", Phys. Rev. Lett. **73**, 676 (1994).
[Ter05] J. Tersoff, M. Freitag, J. C. Tsang, and Ph. Avouris, "Device modeling of long-channel nanotube electro-optical emitter", Appl. Phys. Lett. **86**, 263108 (2005).
[Ter07] J. Tersoff, "Low-frequency noise in nanoscale ballistic transistors", Nano Lett. **7**, 194 (2007).
[The96] A. Thess, R. Lee, P. Nikolaev, H. Dai, P. Petit, J. Robert, C. Xu, Y. H. Lee, S. G. Kim, A. G. Rinzler, D. T. Colbert, G. E. Scuseria, D. Tománek, J. E. Fischer, R. E. Smalley, "Crystalline ropes of carbon nanotubes", Science **273**, 483 (1996).

[Tom00] T.W. Tombler, C. Zhou, L. Alexseyev, J. Kong, H. Dai, L. Liu, C. S. Jayanthi, M. Tang, S-Y Wu, "Reversible electromechanical characteristics of carbon nanotubes under local-probe manipulation", Nature **405**, 769 (2000).
[Val06] L. Valentini, F. Mengoni, I. Armentano, J. M. Kenny, L. Ricco, J. Alongi, M. Trentini, S. Russo, A. Mariani, "Enhancement of photoelectrical properties in polymer nanocomposites containing modified single-walled carbon nanotubes by conducting dendrimer", J. Appl. Phys. **99**, 114305 (2006).
[Vin02] P. Vincent, S. T. Purcell, C. Journet, V. T. Binh, "Modelization of resistive heating of carbon nanotubes during field emission", Phys. Rev. B **66**, 075406 (2002).
[Vit99] A. De Vita, J. C. Charlier, X. Blase, and R. Car, "Electronic structure at carbon nanotube tips", Appl. Phys. A **68**, 283 (1999).
[Wan98] Q. H. Wang, A. A. Setlur, J. M. Lauerhaas, J. Y. Dai, E. W. Seelig, and R. P. H. Chang, "A nanotube-based field-emission flat panel display", Appl. Phys. Lett. **72**, 2912 (1998).
[Wan05] F. Wang, G. Dukovic, L. E. Brus, T. F. Heinz, "The optical resonances in carbon nanotubes arise from excitons", Science **308**, 838 (2005).
[Wei01] B. Q. Wei, R. Vajtai, and P. M. Ajayan, "Reliability and current carrying capacity of carbon nanotubes", Appl. Phys. Lett. **79**, 1172 (2001).
[Wei04] J. Wei, H. Zhou, D. Wu, B. Wei, "Carbon nanotube filaments in household light bulbs", Appl. Phys. Lett. **84**, 4869 (2004).
[Wei07b] W. Wei, Y. Liu, Y. Wei, K. Jiang, L.-M. Peng, and S. Fan, "Tip cooling effect and failure mechanism of field-emitting carbon nanotubes", Nano Lett. **7**, 64 (2007).
[Whi93] C. T. White, D. H. Robertson, and J. W. Mintmire, "Helical and rotational symmetries of nanoscale graphitic tubules", Phys. Rev. B **47**, 5485 (1993).
[Whi98] C. T. White and T. N. Todorov, "Carbon nanotubes as long ballistic conductors", Nature **393**, 240 (1998).
[Whi05] C. T. White and J. W. Mintmire, "Fundamental properties of single-wall carbon nanotubes ", J. Phys. Chem. B **109**, 52 (2005).
[Wil98] J. W. G. Wildöer, L. C. Venema, A. G. Rinzer, R. E. Smalley, C. Dekker, "Atomic structure of atomically resolved carbon nanotubes", Nature **391**, 59 (1998).
[Xu92] C. H. Xu, C. Z. Wang, C. T. Chan, and K. M. Ho, J. Phys.: Condens. Matter **4**, 6047 (1992).
[Xue99] Y. Xue and S. Datta, "Fermi-level alignment at metal-carbon nanotube interfaces: application to scanning tunneling spectroscopy", Phys. Rev. Lett. **83**, 4844 (1999).
[Yai04] Y. Yaish, J.-Y. Park, S. Rosenblatt, V. Sazonova, M. Brink, P. L. McEuen, "Electrical nanoprobing of semiconducting carbon nanotubes using an atomic force microscope", Phys. Rev. Lett. **92**, 046401 (2004).
[Yan99] L. Yang, M. P. Anantram, J. Han and J. P. Lu, "Band-gap change of carbon nanotubes: Effect of small uniaxial and torsional strain", Phys. Rev. B **60**, 13874 (1999).
[Yan00] L. Yang and J. Han, "Electronic structure of deformed carbon nanotubes", Phys. Rev. Lett. **85**, 154 (2000).
[Yan02] C. K. Yang, J. Zhao, and J. P. Lu, "Binding energies and electronic structures of adsorbed titanium chains on carbon nanotubes", Phys. Rev. B **66**, 041403(R) (2002).
[Yao99] Z. Yao, H. W. Ch. Postma, L. Balents, C. Dekker, Nature **402**, 273 (1999).

References

[Yao00] Z. Yao, C. L. Kane, and C. Dekker, "High-field electrical transport in single-wall carbon nanotubes", Phys. Rev. Lett. **84**, 2941 (2000).
[Yoo02] Y.-G. Yoon, P. Delaney, and S. G. Louie, "Quantum conductance of multiwall carbon nanotubes", Phys. Rev. B **66**, 073407 (2002).
[Yue02] G. Z. Yue, Q. Qiu, Bo Gao, Y. Cheng, J. Zhang, H. Shimoda, S. Chang, J. P. Lu, and O. Zhou, "Generation of continuous and pulsed diagnostic imaging x-ray radiation using a carbon-nanotube-based field-emission cathode", Appl. Phys. Lett. **81**, 355 (2002).
[Zha99] Y. Zhang, T. Ichihashi, E. Landree, F. Nihey, and S. Iijima, "Heterostructures of single-walled carbon nanotubes and carbide nanorods", Science **285**, 1719 (1999).
[Zha04] H. Zhao and S. Mazumdar, "Electron-electron interaction effects on the optical excitations of semiconducting single-walled carbon nanotubes", Phys. Rev. Lett. **93**, 157402 (2004).
[Zha05] J. Zhang, G. Yang, Y. Cheng, B. Gao, Q. Qiu, Y. Z. Lee, J. P. Lu, and O. Zhou, "Stationary scanning x-ray source based on carbon nanotube field emitters", Appl. Phys. Lett. **86**, 184104 (2005).
[Zha06] J. Zhang, A. Boyd, A. Tselev, M. Paranjape, and P. Barbara, "Mechanism of NO_2 detection in carbon nanotube field effect transistor chemical sensors", Appl. Phys. Lett. **88**, 123112 (2006).
[Zhe03] M. Zheng, A. Jagota, M. S. Strano, A. P. Santos, P. Barone, S. G. Chou, B. A. Diner, M. S. Dresselhaus, R. S. McLean, G. B. Onoa, G. G. Samsonidze, E. D. Semke, M. Usrey, D. J. Walls, "Structure-based carbon nanotube sorting by sequence-dependent DNA assembly", Science **302**, 1545 (2003).
[Zhe04] X. Zheng, G. Chen, Z. Li, S. Deng, N. Xu, "Quantum-mechanical investigation of field-emission mechanism of a micrometer-long single-walled carbon nanotube". Phys. Rev. Lett. **92**, 106803 (2004).
[Zho00] C. Zhou, J. Kong, E. Yenilmez, and H. Dai, "Modulated chemical doping of individual carbon nanotubes", Science **290**, 1552 (2000).
[Zho05] X. Zhou, J.-Y. Park, S. Huang, J. Liu, and P. L. McEuen, "Band structure, phonon scattering, and the performance limit of single-walled carbon nanotube transistors", Phys. Rev. Lett. **95**, 146805 (2005).

Index